

Aus der Klinik und Poliklinik für Kinder- und Jugendmedizin
(Gf. Direktor Univ.- Prof. Dr. med. Holger N. Lode)
der Universitätsmedizin Greifswald

Immune response and outcome of high-risk neuroblastoma patients immunized with anti-
idiotypic antibody ganglidiomab: a compassionate use program

Inaugural - Dissertation

zur

Erlangung des akademischen Grades

Doktor der Medizin
(Dr. med.)

der Universitätsmedizin

der Universität Greifswald

2021

vorgelegt von
Leah Bernadette Klingel

Dekan: Prof. Dr. Karlhans Endlich

Gutachter/innen:

1. Prof. Dr. Holger Lode

2. PD Dr. Patrick Hundsdörfer

Tag der Disputation: 19.01.2022

For Charles

Abstract

Background and Aim: High-risk neuroblastoma (HR-NB) is associated with a dismal prognosis despite the utilization of multimodal treatment, including therapy with an anti-GD2 monoclonal antibody (mAb). Here we investigated the use of an anti-idiotypic vaccine (ganglidiomab) in patients with HR-NB with or without relapse. Ganglidiomab is a murine monoclonal anti-idiotypic antibody and a structural mimic of GD2.

Patients and Methods: In this compassionate use program, seven HR-NB patients (two with relapsed disease) who achieved complete remission after salvage therapy were enrolled. They received 6-22 subcutaneous vaccine injections every two weeks. Each subcutaneous vaccine injection consisted of 0.5mg of ganglidiomab with 1.67mg aluminum as adjuvant. The immune response was quantified by ELISA methods. We investigated the vaccine-induced antibody response against ganglidiomab (vaccine), against ganglidiximab (a human-mouse chimeric variant of ganglidiomab), as well as against GD2, in immunized patients and determined the time to relapse or progression to last follow-up.

Results: Among the patients enrolled, 6/7 showed an immune response against ganglidiomab as well as an anti-ganglidiximab seroconversion. The non-responding patient had a haploidentical stem cell transplantation as part of the previous treatment, which is associated with B-cell immunodeficiency. However, an anti-GD2 seroconversion was only seen in 2/7 patients. Common toxicities were self-limited, including injection-related local reactions. No fever, pain, neuropathy, or grade 3/4 toxicities occurred during or post-treatment. All immunized patients did not experience a relapse or progression of their neuroblastoma with a median range of 56 months and 16 days from the first vaccine dose to the last follow-up, which contrasts with what is expected from historical control cohorts.

Conclusions: This is the first in man use of the anti-idiotypic vaccine ganglidiomab in HR-NB patients. The vaccine was well-tolerated, and none of the vaccinated patients experienced a relapse or progression. These findings provide an important basis for the design of prospective clinical trials.

Table of Contents

Abstract	4
List of Tables	7
List of Figures	8
Abbreviations	9
1. Introduction	11
1.1. <i>Embryonal and genetic origins of neuroblastoma</i>	11
1.2. <i>Clinical features of neuroblastoma based on cellular origin</i>	12
1.3. <i>Risk-group stratification in neuroblastoma</i>	14
1.4. <i>Immunobiology of neuroblastoma</i>	16
1.5. <i>Immunotherapy of neuroblastoma</i>	17
1.5.2. <i>Active immunotherapy of neuroblastoma</i>	27
2. Objectives	34
3. Methods and patients	35
3.1. <i>Preparation of the vaccine</i>	35
3.2. <i>Vaccination schedule</i>	35
3.3. <i>Patient characteristics</i>	36
3.4. <i>Side effects of the vaccine</i>	40
3.5. <i>Determination of immune response</i>	41
3.5.1. <i>Binding of antibodies from serum of immunized patients to ganglidiomab</i>	41
3.5.2. <i>Binding of antibodies from the serum of immunized patients to ganglidiximab</i>	42
3.5.3. <i>Binding of antibodies from the serum of immunized patients to GD2</i>	44
3.5.4. <i>Determination of complement dependent cytotoxicity of immunized patients</i>	46
4. Results	47
4.1. <i>Analysis of raw data of patient SL as an example</i>	47
4.1.1. <i>Anti-ganglidiomab immune response of SL</i>	47
4.1.2. <i>Anti-ganglidiximab immune response of SL</i>	51
4.1.3. <i>Anti-GD2 Immune response of SL</i>	54
4.2. <i>Immune response of all patients immunized with ganglidiomab</i>	57
4.2.1. <i>Anti-ganglidiomab immune response of all patients</i>	57
4.2.2. <i>Anti-ganglidiximab immune response of all patients</i>	58
4.2.3. <i>Anti-GD2 immune response of all patients</i>	59
4.2.4. <i>Complement dependent cytotoxicity of all patients</i>	60
4.2.5. <i>Mean CDC activity of all patients</i>	61
4.2.6. <i>Survival of immunized patients</i>	62
5. Discussion	63
5.1. <i>Passive Immunotherapy</i>	64
5.2. <i>Combination immunotherapies with anti-GD2-antibodies</i>	64
5.3. <i>Adoptive transfer of GD2 specific chimeric antigen receptor (CAR) T cells</i>	65
5.4. <i>Adaptive immunotherapy using vaccines</i>	66

5.4.1 Vaccines based on gangliosides.....	66
5.4.2 GD2 mimotope vaccines	67
5.5. <i>Methodological challenges for the detection of a GD2 specific immune response</i>	68
5.6. <i>Role of vaccine design to elicit optimal GD2 response</i>	68
5.6.1 Selection of adjuvant	68
5.6.2 Structure of the antigen used for the vaccine (Peptide-mimotopes)	70
5.7. <i>Outcome of patients vaccinated with ganglidiomab</i>	72
6. Summary	73
7. References	75
8. Danksagung	83
9. Eidesstattliche Erklärung.....	84
10. Lebenslauf	85

List of Tables

Table 1. International Neuroblastoma Staging System [29]	15
Table 2. International Neuroblastoma Risk Group Staging System (INRGSS)[29, 34].....	16
Table 3. Time from initial diagnosis to start of vaccination and number of ganglidiomab doses	35
Table 4. Patient characteristics enrolled in the compassionate use program	36
Table 5. Patients' medical history and comorbidities.....	36
Table 6. Treatment received from initial diagnosis to relapse.....	37
Table 7. Optical density signals of varying ch14.18/CHO concentrations in the ganglidiomab ELISA.	48
Table 8. Optical density signals in the ganglidiomab ELISA of serum taken at vaccination time points of patient SL analyzed in quadruplicates.....	49
Table 9. Concentration of the anti-ganglidiomab response in the serum taken at vaccination time points of patient SL analyzed in quadruplicates	50
Table 10. Optical density signals of varying ch14.18/CHO concentrations in the ganglidiximab ELISA.....	51
Table 11. Optical density signals in the ganglidiximab ELISA of serum taken at vaccination time points of patient SL analyzed in quadruplicates	52
Table 12. Concentration of the anti-ganglidiximab response in the serum taken at vaccination time points of patient SL analyzed in quadruplicates	53
Table 13. Optical density signals of different ch14.18/CHO concentrations in the GD2 ELISA	54
Table 14. Optical density signals in the GD2 ELISA of serum taken at vaccination time points of patient SL analyzed in quadruplicates	55
Table 15. Concentration of the anti-GD2 response in the serum taken at vaccination time points of patient SL analyzed in triplicates.....	56
Table 16. Patient status and range of the first vaccine dose to the last follow-up	63

List of Figures

Figure 1. Effect of immunotherapy in the International Society of Pediatric Oncology Europe Neuroblastoma Group SIOPEX high-risk neuroblastoma 1 trial (HR-NBL1 trial)25

Figure 2. Jerne's network model of idiotypic interactions using GD2 as an example31

Figure 3. Generation of ganglidiomab through the use of classic hybridoma technology33

Figure 4. Schematic for the detection of an anti-ganglidiomab immune response in the serum of immunized patients.....42

Figure 5. Schematic for the detection of an anti-ganglidximab response in the serum of immunized patients (one-arm principle)44

Figure 6. Schematic for the detection of an anti-GD2 response in the serum of immunized patients45

Figure 7. Complement dependent cytotoxicity in neuroblastoma47

Figure 8. Standard curve representing the detectable concentration range for the detection of an anti-ganglidiomab response.....49

Figure 9. Standard curve representing the detectable concentration range of anti-ganglidximab52

Figure 10. Standard curve representing the detectable concentration range of the anti-GD2 response55

Figure 11. Induction of anti-ganglidiomab humoral response after vaccination with ganglidiomab over time ...58

Figure 12. Induction of anti-ganglidximab humoral response after vaccination with ganglidiomab over time ..59

Figure 13. Induction of anti-GD2 humoral response after vaccination with ganglidiomab over time60

Figure 14. CDC activity in the sera of immunized patients61

Figure 15. Mean CDC activity in the sera of all immunized patients62

Abbreviations

Ab	Antibody
ADCC	Antibody-dependent Cell-mediated Cytotoxicity
ALK	Anaplastic Lymphoma Kinase
APC	Antigen Presenting Cell
ASCT	Autologous Stem Cell Transplantation
ASD	Atrial Septum Defect
BSA	Bovine Serum Albumin/Body Surface Area
BuMel	Busulfan and Melphalan
CART	Chimeric Antigen Receptor (CAR) T cells
CD	Cluster of Differentiation
CD4/8	Cluster of Differentiation 4/8
CDC	Complement Dependent Cytotoxicity
CHO	Chinese Hamster Ovary
COG	Children's Oncology Group
COJEC	Cisplatin, Vincristine, Carboplatin, Etoposide and Cyclophosphamide
CP	Control Population
CTCAE	Common Terminology Criteria for Adverse Events
EFS	Event-free Survival
ELISA	Enzyme-linked Immunosorbent Assay
EMA	European Medicines Agency
EpCAM	Epithelial Cell Adhesion Molecule
ESBL	Extended Spectrum Beta Lactamase
EU	European Union
Fab	Antigen-binding Fragment
GD2	Disialoganglioside
GM-CSF	Granulocyte-Macrophage Colony-Stimulating Factor
GPOH	Gesellschaft für Pädiatrische Onkologie und Hämatologie
GvHD	Graft versus Host Disease
HACA	Human anti-Chimeric Antibody
HAMA	Human anti-Mouse Antibody
HLA	Human Leucocyte Antigen
HMW-MAA	High Molecular Weight-Melanoma Antigen
HR-NB	High-risk Neuroblastoma
HRP	Horseradish Peroxidase
IFA	Incomplete Freund's Adjuvant
IL-2	Interleukin-2
KLH	Keyhole Limpet Hemocyanin
INRG	International Neuroblastoma Risk Group
INSS	International Neuroblastoma Staging System
IP	Immunotherapy Population
LOD	Limits of Detection
MAC	Membrane Attack Complex
MAPK	Mitogen-activated Protein Kinase
MEC	Melphalan, Etoposide, and Carboplatin
MHC	Major Histocompatibility Complex
MIBG	Metaiodobenzylguanidine

MRD	Minimal Residual Disease
MWCO	Molecular Weight Cut-off
NANA	N-acetylneuraminic acid
NB	Neuroblastoma
OD	Optical Density
OS	Overall Survival
PAMAM	Polyamidoamine
PBS	Phosphate-buffered Saline
PD	Pharmacodynamics
PD1	Programmed Cell Death 1
PFS	Progression-free Survival
PK	Pharmacokinetics
PHOX 2b	Paired-like Homeobox 2b
QC	Quality Control
RA	Retinoic Acid
RAP1	Ras-related Protein 1
RIST	Rapamycin, Dasatinib, Irinotecan, and Temozolomide
RT	Room Temperature
SIOPEN	Society of Pediatric Oncology Europe Neuroblastoma Group
SPOT	Synthetic Peptide Arrays on Membrane Supports
TAA	Tumor Associated Antigen
TACE	Transarterial Chemoembolization
TBI	Total Body Irradiation
TMB	Tetramethylbenzidine
TMG	Tumor Marker Gangliosides
TTP	Time to Progression
US FDA	United States Food and Drug Administration
VIP	Vasoactive Intestinal Peptide
VRE	Vancomycin Resistant Enterococcus

1. Introduction

The standard regimen of high-intensity chemotherapy, surgery, myeloablative therapy with autologous stem cell rescue, radiation therapy, and MIBG treatment have not been successful in reducing relapse rates in high-risk neuroblastoma patients [1]. Treatment options for this malignancy, the most common extracranial, solid childhood tumor, has thus seen an array of novel and scientific advancements in immunotherapy in the past few years [2, 3].

The emergence of these innovative antibody and cell-mediated immunotherapeutic agents has resulted in many clinical trials dedicated to relapsed neuroblastoma patients. Studies investigating the molecular and genetic profiles of tumors and their aberrations are also currently ongoing. Combining these new therapeutics with the existing treatment regimen will be imperative to improve the poor outcomes of patients with relapsed and refractory high-risk neuroblastoma [1].

Neuroblastoma indeed remains to be a complex disease to treat, particularly since approximately half of all patients will be stratified into the high-risk group at the time of diagnosis [4]. Also, the event-free survival (EFS) rate at three years for patients undergoing a multimodal treatment regimen is below 50% [5]. Affected children thus bear a dismal prognosis [6]. This poor outcome has led to the development of new therapeutic strategies, including immunotherapies of advanced neuroblastoma.

1.1. Embryonal and genetic origins of neuroblastoma

The quest to understand the origin of neuroblastoma has resulted in the study of two candidate genes that seem to play a crucial role in the origin of this disease. Research on familial neuroblastoma, comprising 2% of all neuroblastomas, have illustrated a gene mutation (PHOX2b - Paired-like homeobox 2b) that has been linked to the emergence of this malignancy [7]. This gene plays an essential role in the growth and development of autonomic neurons derived from the neural crest. It also encodes a transcription factor that stimulates cell cycle exit and neuronal differentiation [2, 8]. A more common genetic aberration in

neuroblastoma can be found in the ALK (anaplastic lymphoma kinase) receptor tyrosine kinase gene. ALK is generally found in the evolving sympathoadrenal lineage of the neural crest [9]. It is known to regulate the balance between the proliferation and differentiation of cells through the mitogen-activated protein kinase (MAPK) and the Ras-related protein 1 (RAP1) signal transduction pathways. There is also evidence suggesting that PHOX2b can directly regulate ALK gene expression [2].

Sporadic neuroblastomas, on the other hand, have rare mutations of the PHOX2B gene. Instead, 6-10% of neuroblastomas carry a somatic ALK activating mutation, and a further 3-4% have high-level ALK gene amplification [10]. These results indicate that ALK is a main oncogenic driver in neuroblastoma, and mutations in the ALK gene are correlated with a deadly disease [2, 11]. ALK has thus been the subject of several preclinical studies focusing on molecular therapy [12].

However, the most frequent genetic abnormality in sporadic neuroblastoma is the amplification of MYCN, which is seen in nearly 22% of tumors and is associated with a poor outcome [13]. MYCN is known to regulate the growth, differentiation, and survival of cells in the developing nervous system. It is expressed in the maturing neural crest cells and is controlled through several signaling pathways [2]. MYCN is also associated with an invasive and metastatic behavior contributing to all phases of metastasis, that is, adhesion, motility, invasion, and degradation of surrounding tissue [14].

1.2. Clinical features of neuroblastoma based on cellular origin

The cellular origin of neuroblastoma stems from the sympathoadrenal lineage of the neural crest during development [15], thus explaining the typical primary sites as well as the cellular and neurochemical characteristics of neuroblastoma. Most neuroblastoma cases are diagnosed in the abdomen and the thorax, either originating from the adrenal gland or the sympathetic ganglia [2, 16]. However, it can arise anywhere where sympathetic nervous tissue is present.

Approximately 65% of children present with a tumor in the abdominal region, often described as a painless mass. Other typical sites of appearance include the head and neck, chest, and the paraspinal area. Thoracic tumors may also occur and can be found incidentally on chest radiography [17]. On some occasions, patients can present with cervical manifestations, a clinical entity known as Horner's syndrome [18]. A superior vena cava syndrome, a rare manifestation of malignant disease in children, can sometimes also occur [19].

One of the challenges with neuroblastoma is the high rate of metastases at diagnosis [20]. Because of its aggressive nature, it accounts for nearly 15% of all pediatric cancer mortalities [21]. A particular subtype of metastatic neuroblastoma in infants (age 12-18 months) presents with a different clinical picture compared to toddlers or older children. Patients of this subtype often have hepatomegaly with or without pulmonary insufficiency [22]. Young infants can also present with bluish, non-tender, subcutaneous nodules ("blueberry muffin sign"). This cutaneous metastatic pattern is often considered a hallmark of the disease [23]. Nevertheless, the outcome for affected infants remains excellent even without therapeutic intervention due to a high rate of spontaneous regressions observed in this population [24].

This type of metastatic disease in infants, therefore, needs to be distinguished from high-risk metastatic neuroblastoma, which has a poor outcome.

Indicators of metastatic disease include anorexia, bone pain, irritability, fever, pallor, and hypertension. Periorbital ecchymosis, also known as the "raccoon eye sign," is caused by the infiltration of tumors in this area [25]. Children may also become symptomatic from the release of catecholamines from tumor cells, resulting in flushing, sweating, headache, palpitations, and hypertension.

About 5% of children may present with symptoms of spinal cord compression [26]. This emergency occurs in paraspinal neuroblastoma and presents as weakness in the lower extremities accompanied by bowel and bladder dysfunction, back pain, and sensory loss [17].

Of note are distinct paraneoplastic syndromes that are associated with this disease. An example of these is the release of a vasoactive intestinal peptide (VIP) from malignant cells,

resulting in intractable, watery diarrhea, hypokalemia, and poor growth [27]. Another is the opsoclonus–myoclonus syndrome, characterized by the appearance of rapid, involuntary eye movements in all directions of gaze with irregular, frequent muscle jerking and ataxia [28]. Patients with these signs and symptoms usually have a benign disease with favorable biological features.

1.3. Risk-group stratification in neuroblastoma

A distinguishing trait of neuroblastoma is its clinical and molecular heterogeneity. In the current staging system, children with low-risk disease may undergo observation or surgical resection, whereas those with intermediate-risk disease receive chemotherapy and undergo surgery. In contrast, high-risk disease patients receive multimodal intensive treatment, which includes chemotherapy, surgery, myeloablative chemotherapy with autologous stem cell rescue, radiation, and immunotherapy with an anti-GD2 antibody [29, 30]. Therefore patients must be correctly risk-stratified to ensure that they will be receiving the optimal therapy. This system was developed over decades, and the most recent update was put in place in 2009.

In 1971 a staging system was proposed by Evans based on both the site of origin and the clinical behavior of the tumor [31]. This system included a IV-S category to incorporate a set of very young patients (age below 12-18 months) known to have better outcomes despite the presence of metastatic disease to the liver, skin, and bone marrow [29].

In the years to follow, an international group of neuroblastoma experts gathered and developed a surgical staging system to compare outcomes and therapies between countries since numerous staging schemes were being used worldwide [29, 32]. The International Neuroblastoma Staging System (INSS) was then established, taking into account the degree of tumor resection, presence of involved ipsilateral or contralateral lymph nodes, tumor infiltration across the midline of the body, and separation of patients with INSS stage 4S (infants with metastases limited only to the liver, skin, and bone marrow) from other children with metastatic disease (INSS stage 4) to unify staging across groups (see Table 1) [32]. Also, patients with INSS stage 4 were noted to have reduced survival rates than those with stages 1, 2, 3, or 4S disease [33].

Table 1. International Neuroblastoma Staging System [29]

INSS Stage	Description
1	Localized tumor, grossly resected, no lymph node involvement
2A	Unilateral tumor, incomplete gross excision, negative lymph nodes
2B	Unilateral tumor with positive ipsilateral lymph nodes
3	Tumor infiltrating across midline or unilateral tumor with contralateral lymph nodes or midline tumor with bilateral lymph nodes
4	Distant metastatic disease
4S	Localized primary tumor as defined by stage 1 or 2 in patient under 12 months with dissemination limited to the liver, skin, and/or bone marrow (<10% involvement)

In 2005 staging for this disease was renewed during a convention of the International Neuroblastoma Risk Group (INRG) task force and a system using image-defined risk factors instead of the degree of surgical resection was established (INRG Staging System, or INRGSS) [29, 34]. This change allowed for a pretreatment staging of newly diagnosed patients.

The INRGSS was based on analyses of data compiled from more than 8,800 patients from North America, Europe, Japan, and Australia. This classification uses seven prognostic risk factors to delineate the 16 pretreatment groups stratified by these markers. The 8,800 patients were classified as belonging to a very low-, low-, intermediate-, or high-risk group, based on the 5-year event-free survival (EFS) rates of the 16 pretreatment groups [30, 35]. As the surgical and pathologic criteria used to define the old INSS stage are no longer suitable with the pretreatment classification, this new staging system was developed [34].

The INRG staging system is based on imaging criteria, and the degree of local disease is determined by the absence or presence of image-dependent risk factors. Stage M, for instance, means the presence of disseminated disease, similar to INSS stage 4, and stage MS is analogous to INSS stage 4S tumors, with metastases limited to the liver, skin, and bone marrow without cortical bone involvement, but with no restriction on the size of the primary tumor [30]. In addition to incorporating radiographic findings, a few other changes were implemented in the INRG system, including the withdrawal of lymph node assessment and the midline feature of tumors and the use of 18 months instead of 12 months to define MS

disease [29]. The INRGSS (see Table 2) is currently being integrated into new guidelines developed by pediatric oncology groups such as the Children’s Oncology Group (COG) and the SIOPEN (International Society of Pediatric Oncology Europe Neuroblastoma) group.

Table 2. International Neuroblastoma Risk Group Staging System (INRGSS)[29, 34]

INRG Stage	Description
L1	Localized tumor with no image-defined risk factors
L2	Localized tumor with one or more image-defined risk factors
M	Distant metastatic disease
MS	Metastatic disease in children under 18 months with metastases limited to skin, liver, and/or bone marrow (<10% involvement)

The INRG Task Force also established consensus guidelines for detecting minimal disease in bone marrow, blood, and stem-cell preparations, molecular diagnostics, as well as imaging and staging techniques [36-38]. At the time the INRG classification system was developed, DNA copy number alteration analyses and gene expressions were not widely available, and only a few genetic alterations were included in the system. The task force is nevertheless aware of genetic-based studies, which had led to powerful new predictors of outcome. It is thereby expected that the ensuing INRG classification system will give a more accurate prognosis by including profiles of the neuroblastoma genome, transcriptome, and epigenome [30].

1.4. Immunobiology of neuroblastoma

The earliest evidence of a natural immune response against neuroblastoma was described in 1968 when blood lymphocytes, from a group of patients with neuroblastoma, were shown to inhibit colony formation by neuroblastoma cells that had been previously cultured before testing [39, 40]. These lymphocytes were able to prevent colony formation by autologous neuroblastoma cells as well as colony formation by allogeneic neuroblastoma cells. These findings were in contrast to the effect on autologous fibroblasts, which were not affected. Plasma samples were taken from the same patients also hindered tumor cell colony formation in the presence of complement [40].

Primary tumors were also reported to contain leukocytes, and some were seen to regress spontaneously [41]. These studies helped establish the premise that the immune system could develop an anti-neuroblastoma response that can induce cytotoxic lymphocytes against existing neuroblastoma cells. The importance of the lymphocyte's role is further supported by the fact that both tumor lymphocytic infiltrates and higher blood lymphocyte counts at diagnosis correspond with improved survival rates [42]. However, the technology available at this time was not adequate to characterize the cellular or molecular basis for the observations, and so absolute conclusions could not be reached.

In summary, these findings suggest that neuroblastoma activates the cellular and humoral arms of the immune system.

1.5. Immunotherapy of neuroblastoma

Based on the observation that neuroblastoma is not an immunologically inert tumor, the development of immunotherapeutics for this disease advanced over the years.

1.5.1. Passive immunotherapy

The first clinically effective immunotherapy of neuroblastoma is based on passive immunotherapy using monoclonal antibodies against disialoganglioside (GD2). This strategy led to the approval of two antibodies in the United States (dinutuximab) and Europe (dinutuximab-beta), which are both derived from the sequence of anti-GD2 antibody ch14.18. The following sections describe the rationale, mechanisms and clinical findings of this approach:

Disialoganglioside GD₂

Ernst Klenk, a German biochemist, discovered in 1942 a group of carbohydrate-rich glycolipids derived from ganglion cells and called them 'gangliosides' [43]. Gangliosides are made up of glycosphingolipid and sialic acids (N-acetylneuraminic acid, Neu5Ac or NANA), which are nine-carbon monosaccharides. The nomenclature for gangliosides is dependent on the number and position of the NANA residues [44]. Disialogangliosides, GD₂, are biosynthesized from

precursor gangliosides GD3/GM3 by β -1,4-N-acetylgalactosaminyltransferase (GD2 synthase) [45] and are also sialic acid-containing glycosphingolipids commonly found on a cell's outer membrane [46].

The epitope of GD2, where most antibodies are attached to, is located at the end-terminal of the penta-oligosaccharide. GD2 is expressed prenatally on neural and mesenchymal stem cells and is postnatally confined to the central nervous system, peripheral neurons, and skin melanocytes [47].

Considering its immunogenicity, pervasiveness among human cancers, number of epitopes, and location of antigen expression, GD2 was identified as a tumor-associated antigen (TAA). Its high expression on malignant cells such as neuroblastoma and its low and restricted expression on normal tissue characterized GD2 as a suitable target for immunotherapeutic approaches. GD2 was ranked 12th out of 75 potential tumor immunotherapy targets by the National Cancer Institute program for prioritizing cancer antigens [48]. It has become the subject of several trials in recent years, maximizing the potential of immunotherapy among pediatric solid tumors.

GD2 can be found in several embryonal cancers, bone tumors, soft tissue sarcomas, neural crest-derived tumors, and even breast cancer. GD2 expression in these tumor cells is dependent on the activity of the enzyme GM2/GD2 synthase and the number of its existing precursor ganglioside GD3. Neuroblastoma cells, in particular, have high levels of the GM2/GD2 synthase transcript, enzyme activity, and GD2 expression [49, 50]. GD2 expression is correlated with the tumor's proliferation, invasion, and motility abilities [51]. In contrast, the enzyme GM2/GD2 synthase, which is in charge of making GD2, has been utilized as a measure of minimal residual disease (MRD) in the bone marrow, with significant consequences on patient survival [50, 52, 53].

Anti-GD2 antibodies of the 14.18 and the 3F8 family

Murine anti-GD2 mAbs have been described as early as the 1980s for the treatment of cancer. Several anti-GD2 antibodies have since then been characterized, and their structures analyzed

[50, 54]. Anti-GD2 mAbs can identify GD2 positive tumor cells through immunocytology and GD2 positive tumors in patients by immunoscintigraphy. In neuroblastoma, GD2 is an ideal target for therapy as it is abundantly (10^7 molecules per cell [55]) found on tumor cells and forms a stable complex once it binds to an antibody [50]. Moreover, loss of the GD2 antigen from tumors rarely happens as an escape mechanism after receiving antibody therapy. The inactivation of the GD2/GM2 synthase is thus not compatible with tumor survival. Despite this feature, the human brain is protected against parenteral anti-GD2 mAb because of the blood-brain barrier, even though GD2 is expressed by neurons [56].

Anti-GD2 mAb can mobilize human leukocytes to execute antibody-dependent cell-mediated cytotoxicity (ADCC) and monocyte-macrophage-mediated phagocytosis [2, 57]. When the Fc receptors on granulocytes and natural killer (NK) cells are activated by the mAb attached to the tumor cells, cytotoxic granules and cytokines are discharged, thereby killing the tumor cell through ADCC. Furthermore, these Fc-receptors also induce phagocytosis by stimulating monocytes and macrophages [2].

In addition to ADCC, the complement dependent cytotoxicity (CDC) is a key effector function of mAbs. When complement C1q attaches to the Fc portion of a tumor-bound mAb, it starts a complement activation cascade prompting the generation of a membrane attack complex (MAC), leading to the creation of pores in the cell membrane and the lysis of tumor cells. [2, 50]. Although neuroblastoma patients receiving high-dose chemotherapy show an attenuated lymphocyte response, neutrophils and macrophages are only temporarily deactivated. Hence, CDC and ADCC, which rely on these effector cells, can still mediate tumor cell eradication. Also, the relative absence of complement-inhibitory proteins on the tumor cell surface makes them more receptive to the effects of ADCC and CDC [58, 59]. In addition, non-immune mediated anti-tumoral effects are also induced by anti-GD2 mAbs, such as anoikis. Anoikis is a process where adherent cells are disengaged from the extracellular matrix leading to apoptosis by detached cells, a mechanism that anti-GD2 mAbs may enhance [46]. There is also emerging evidence that anti-GD2 mAbs work by inhibiting the activation of an intracellular signal transduction pathway (PI3K/Akt), resulting in reduced viability via induction of apoptosis and thereby reduced invasiveness of cancer cells [60].

In the 1980s, murine IgG3 antibody 3F8 was tested in the first human Phase I clinical trial among neuroblastoma and melanoma patients [50, 61]. From this study, major side effects of pain, fever, hypertension, and urticaria were observed and were shown to have a severe course if not controlled early. Pain side effects, however, was not associated with the 3F8 dose or the duration of the 3F8 infusion [62].

Also identified in this trial is the level of serum human anti-mouse antibody (HAMA) in some of the patients, with those having HAMA complaining of minimal side effects during a 3F8 infusion [61]. In the subsequent Phase II studies of 3F8, antitumor effects were detected, especially when combined with granulocyte-macrophage colony-stimulating factor (GM-CSF). Cytokines such as GM-CSF and Interleukin-2 (IL-2) have been shown to enhance the effects of ADCC. GM-CSF works by activating clonal expansion and maturation of progenitor cells in the granulocyte-macrophage pathways to form granulocytes, monocytes, macrophages and dendritic cells. Furthermore, it indirectly stimulates T cell activation via secretion of tumor necrosis factor, interferon, and IL-1 [46, 63]. IL-2, on the other hand, is known to regulate T and B cells, and activate the growth of monocytes, macrophages and NK cells [64]. 3F8 combined with GM-CSF seem to enhance the long-term survival of HR neuroblastoma patients. Before the introduction of immunotherapy, the 5-year event-free survival (EFS) was only 13-30% in HR neuroblastoma, whereas the 5-year progression-free survival (PFS) of the same patient population treated with 3F8 and GM-CSF in first remission increased to 56-62% [53, 65, 66].

Clinical findings with ch14.18

Despite being tolerated well and having proven anti-neuroblastoma activity, the hypersensitivity side effect and the development of HAMA from the use of murine anti-GD2 mAbs often restrict its repeated use. To reduce HAMA, chimeric (murine human) and humanized anti-GD2 mAbs were developed. Chimeric 14.18 (ch14.18) was created by fusing the constant regions of the human gamma 1 heavy chain and the human kappa light chain with the heavy- and light-chain variable regions of mouse 14.18 [50, 67].

This human-murine chimeric antibody was subsequently renamed dinutuximab, and it was produced in murine non-secreting myeloma cells SP2/0. Compared to the previous mAbs,

dinutuximab maintained high anti-GD2 specificity, had equal CDC and 50-100 fold higher ADCC [67] compared to the murine version. A typical and expected on target off tumor side effect observed in phase I clinical trials is the induction of neuropathic pain, which occurs with all anti-GD2 antibodies. Further side effects were hypertension, fever and allergic reactions. Cases of peripheral motor neuropathy and transverse myelitis have also been reported [68]. In order to improve the efficacy of therapy with ch14.18, cytokine co-mediation was introduced very early in the clinical development in order to enhance the ADCC effector function. The inclusion of GM-CSF into the treatment regimen did not worsen the mentioned side effects, however IL-2 resulted in the emergence of inflammatory toxicities, namely capillary leak syndrome and hepatic transaminitis. Finally, a dinutuximab dose of 20mg/m²/day for 5 days was established and further tested in combination with GM-CSF and IL-2 [69].

The efficacy of ch14.18 was tested in two large clinical trials in high-risk neuroblastoma patients who responded to frontline induction and consolidation therapy. In the German neuroblastoma non-randomized trial, dinutuximab was given to all patients after stem cell transplant, and results were compared to maintenance chemotherapy from a different treatment era. Patients treated with dinutuximab did not have better EFS rates, but OS at three years was at 68% compared to only 57% and 47% for patients receiving chemotherapy or no further therapy post-transplant, respectively [70].

In the ANBL0032 trial conducted by the Children's Oncology Group (COG), 226 patients with HR neuroblastoma in remission after undergoing chemotherapy and autologous stem cell transplantation (ASCT) were randomized to receive either five cycles of dinutuximab antibody therapy combined with interleukin-2 (IL-2), granulocyte-macrophage colony stimulating factor (GM-CSF) and cis-retinoic acid (RA) or RA alone. Patients administered with immunotherapy received 5 cycles of ch14.18, 3 of which in combination with GM-CSF and the rest with IL-2. At 2 years follow-up, dinutuximab-treated patients had significantly higher EFS (66% vs 46%, p=0.01) and OS rates (86% vs 75%, p=0.02) compared to the RA group. This seminal work confirmed the effectiveness of anti-GD2 immunotherapy and established it as the new standard of care for maintenance therapy among patients with high-risk neuroblastoma (HR-NB) post-ASCT. At 4 years follow-up, EFS rates however were no longer significant although the OS rates remain higher for the immunotherapy group [5, 46, 59].

The US Food and Drug Administration (FDA) and the European Medicines Agency (EMA) approved in 2015 dinutuximab in combination with GM-CSF, IL-2, and RA after undergoing stem cell transplantation for the treatment of HR-NB pediatric patients who at least had a partial response with prior multimodal therapy. The recommended dosage of dinutuximab was 17.5mg/m²/day x 4 days/cycle for 5 cycles [46]. However, the license holder (United Therapeutics) retracted its use, and therefore this treatment consisting of three components (dinutuximab, IL-2, and GM-CSF) is not available in the European Union (EU).

Clinical development of ch14.18/CHO (dinutuximab-beta)

In response to this, a biologically equivalent version of the ch14.18 antibody was developed by European investigators. The main difference compared to the previous versions of ch14.18 antibodies, including dinutuximab, was its production in CHO (chinese hamster ovary) cells. This change in production is associated with a different glycosylation pattern leading to differences in the activity level (ADCC). The remanufactured antibody was designated as ch14.18/CHO (dinutuximab-beta) and was used in clinical trials of the SIOPEN group. The glycosylation pattern unique to CHO ensures its safety, optimizes the patient's biological response, and influences the pharmacokinetics of the immunotherapeutic [71]. From a safety point of view, many viral entry genes are inhibited in CHO cells minimizing the risk of transmitting infections to humans, which is not the case with the ch14.18 produced in SP2/0 cells. Furthermore, CHO cells produce recombinant glycoproteins that are biologically active in humans [71, 72].

In a preclinical study looking into the effector function of the ch14.18/CHO antibody, its specificity to the nominal antigen was shown to translate into a high CDC and ADCC activity against GD2 positive neuroblastoma and melanoma cell lines. In contrast, the chimeric anti-CD20 antibody (Rituximab), which shared the human-mouse chimeric protein structure to the ch14.18 mAb, showed no effect, which proved the antigen specificity of the observed ADCC and CDC responses [73]. Additionally, a comparison of the ch14.18 antibody preparations from SP2/0, NS0, and CHO production cell lines yielded a comparable performance in CDC reactions. However, a superior ADCC activity of ch14.18/CHO over ch14.18/SP2/0 and ch14.18/NS0 was detected at low antibody concentrations [73].

In a phase I clinical trial, ch14.18/CHO was found to have identical pharmacokinetics and toxicity (including the level of neuropathic pain) compared to ch14.18/SP2/0 and is also capable of inducing objective clinical responses in patients with relapsed neuroblastoma [72].

As mentioned previously, one of the complications of the anti-GD2 mAb therapy, not seen with other chimeric mAbs, is the associated neuropathic pain observed during administration. Previous data illustrate that mechanical-allodynia could be secondary to the anti-GD2 antibody's effects on peripheral nerves and, therefore, requires administration of analgesic drugs to ensure completion of the antibody treatment [74]. To improve this side effect, a new delivery method was developed by extending the infusion delivery time of the same cumulative dose of antibody from 5 to 10 days [75].

In a single-center study investigating the long-term infusion of dinutuximab-beta (100mg/m² over ten days) with subcutaneous IL-2, its clinical response, survival, and toxicity were evaluated. The results revealed a reduction in toxicity, such as pain, fever, and allergic reactions under the longer infusion duration, while maintaining its clinical activity and efficacy [75, 76].

Based on these results, dinutuximab-beta (ch14.18/CHO) has been approved in the EU for treating high-risk NB patients, 12 months and older, who have at least partially responded to induction chemotherapy and have received myeloablative chemotherapy [77].

Regarding the use of cytokines, preclinical data indicate that mAbs directed against GD2 have improved activity against NB when combined with GM-CSF or IL-2 (Interleukin-2). A randomized study in patients with HR-NB comparing the addition of dinutuximab, GM-CSF, and IL-2 to oral isotretinoin, versus isotretinoin alone as a treatment for residual disease showed a survival benefit in the immunotherapy group [78]. In this context, however, the exact role of cytokines remained unclear.

In order to understand the role of Interleukin-2, a randomized trial was completed comparing the effect of dinutuximab-beta with and without IL-2 on survival [79]. In this phase 3 clinical trial (HR-NBL1/SIOPEN), the addition of subcutaneous IL-2 (6×10^6 IU/m²) to dinutuximab-beta

(5 x 20 mg/m² per day in an eight-hour infusion) in patients with HR neuroblastoma, who had previously responded to induction and consolidation treatment, did not have any significant effect on EFS or OS, indicating that adding the cytokine IL-2 to frontline therapy with the anti-GD2 antibody ch14.18/CHO provided no extra survival benefit and only added to treatment toxicity of high-risk neuroblastoma patients [78].

Since all patients were treated with dinutuximab-beta in this randomized trial, it was not possible to evaluate the role of dinutuximab-beta for this treatment effect. This was done by comparing the outcome of patients treated with dinutuximab-beta (with and without IL-2) to the outcome of patients in a treatment era where the antibody was not available.

In this report, the introduction of dinutuximab-beta has been shown to increase the chances of survival among high-risk neuroblastoma children. Since dinutuximab-beta is not identical to dinutuximab, the isolation of its positive effects on treatment outcome is an essential milestone [80].

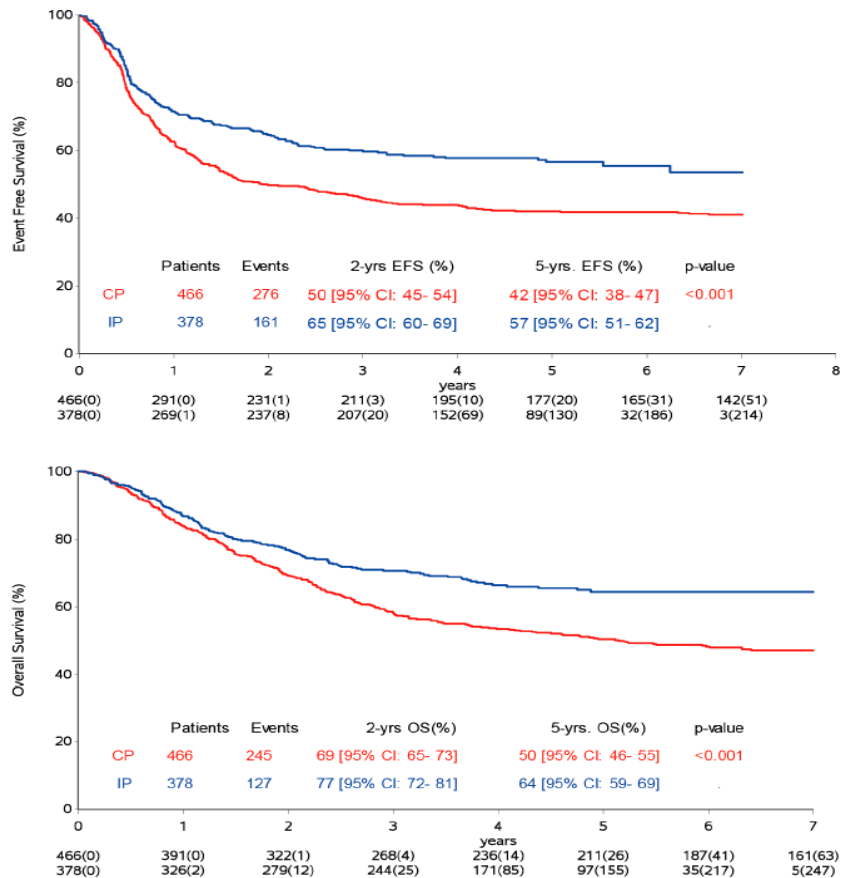


Figure 1. Effect of immunotherapy in the International Society of Pediatric Oncology Europe Neuroblastoma Group (SIOPEN) high-risk neuroblastoma 1 trial (HR-NBL1 trial)

The control population (CP) was prior to the introduction of dinutuximab-beta (red curve) and the immunotherapy population (IP) was after introduction of dinutuximab-beta (blue curve). Figure 1 above shows a Kaplan Meier analysis of event-free (top) and overall (bottom) survival [81].

The treatment-associated toxicity observed for those receiving IL-2 was much higher than those getting the antibody alone. Looking at the Lansky performance scale of patients, a status of 30% or less was seen in 41% vs. 17% of cases in the IL-2 group and antibody alone group, respectively. Also, early termination of therapy and occurrence of fever were noted more frequently in the group receiving IL-2 (39% vs. 15%, 41% vs. 14%; $p < 0.001$) [82]. There were also significantly more allergic reactions and a higher incidence of capillary leak, pain, hypotension, central nervous toxicity, and diarrhea within the IL-2 group.

The toxic effects observed in both treatment groups were nevertheless expected and attributed to the antibody binding to GD2 expressed on normal nerve cells and the cytokine-mediated inflammatory responses (i.e., capillary leak syndrome) [5, 78]. Compared to a

previous study reporting that 25% of participants given dinutuximab (ch14.18/SP2/0) in cycles combined with IL-2 developed anaphylaxis, only 3% of patients receiving dinutuximab-beta and IL-2 had anaphylactic reactions [78]. Recognizing the limitations of comparing cross-trials, this discovery might be due to the absence of the galactose- α -1,3-galactose (α -gal) glycosylation determinant on dinutuximab-beta [83]. As α -gal is a significant carbohydrate in non-primate mammals, and anti- α -gal is a ubiquitous natural immunoglobulin found in humans, α -gal glycosylation of antibodies might increase the possibility of allergic reactions. Murine cell lines, such as SP2/0, are known to mediate α -gal glycosylation, which does not occur with CHO lines [78].

On the other hand, dinutuximab-beta without cytokines was observed to result in objective responses among patients with residual disease. This regimen continues to be the standard maintenance therapy recommended by SIOPEN for high-risk neuroblastoma, although the benefits might be less evident in some subgroups (<1.5 years, *MYCN*-amplified localized disease) [80].

Human anti-chimeric immune response and survival

The treatment with a human-mouse chimeric monoclonal antibody can lead to the induction of human anti-chimeric antibodies (HACA), and is also known to occur for patients treated with ch14.18. A HACA response may affect the pharmacokinetics (PK), pharmacodynamics (PD) as well as the drug's toxicity profile. In order to evaluate the HACA response in patients treated with ch14.18/CHO, a validated ELISA (Enzyme-linked Immunosorbent Assay) method was established [84, 85]. Patients are considered HACA positive once HACA is detected in any serum sample (Limits of Detection (LOD) of HACA-ELISA 1.1 μ g/ml) [84].

The frequency of a HACA response as well as its effect on PK and PD was evaluated in a compassionate use cohort of 53 neuroblastoma patients treated with long-term infusion of dinutuximab-beta in combination with IL-2. In this study, 30/37 patients were labeled HACA-negative and seven patients as HACA-positive (four of which were further classified as HACA-low responders (mean HACA value <10 mg/ml), and the rest as HACA-high responders (mean HACA value \geq 10 mg/ml). As expected, ch14.18/CHO concentrations remained high in the circulation of HACA-negative patients (30/37) during the entire treatment period [76]. In

comparison, the development of HACA resulted in a reduction of Ab levels in each successive treatment cycle among HACA-low responders and HACA-high responders compared to HACA-negative patients [76].

As to the effect of HACA on immune modulation, the administration of ch14.18/CHO in HACA-negative patients resulted in a two-fold increase in ADCC and a four-fold increase in CDC in every treatment cycle compared to the recorded baseline values [86]. On the other hand, HACA-high- and HACA-low responders displayed a significant reduction in CDC starting on day 8 of Ab infusion compared to HACA-negative patients. However, reductions in Ab-dependent cellular cytotoxicity levels compared to HACA-negative patients were not significant [76]. These results highlight that high HACA levels do not always translate to a complete neutralization of the ch14.18/CHO effector functions.

In addition, this study also investigated the formation of GD2-specific Ab in patients who tested positive for HACA using an established method (GD2 solid-phase ELISA). However, the study did not find any anti-GD2-specific signal in any evaluable HACA-positive patient, implying that induction of a GD2-specific anti-anti-Id Ab was not observed [76].

1.5.2. Active immunotherapy of neuroblastoma

One major disadvantage of passive immunotherapy with a monoclonal antibody is the clearance of therapy over time. Therefore, the use of active immunotherapy, i.e., a vaccine which leads to the continuous production of an anti-GD2 antibody in the immunized patient, is an appealing new perspective.

Vaccination with GD2 antigen

Disease recurrence among neuroblastoma and sarcoma patients is usually a consequence of micrometastases that remain undetected as minimal residual disease. In numerous experimental animal models, vaccine-induced antibodies against various surface antigens can protect against the spread of micrometastases and subsequent fatal outcomes [87, 88]. Neuroblastomas, sarcomas, and melanomas express GD2 and GD3 on their cell surface with a limited expression on normal tissue and are therefore suitable targets.

These tumor marker gangliosides (TMG) are essential features of cancer [89]. They are not only tumor-associated antigens, but they are also known to be immunosuppressive [90] as they can suppress antigen presentation [91]. Therefore, targeting gangliosides with antibodies may also activate the host's immune system by removing the ganglioside's immune suppressive function.

Even after therapy, expression of TMGs, at least in osteosarcoma and glioblastoma, does not affect downregulation, making them attractive targets for cancer therapy as they seem less susceptible to genetic instability [92].

However, active immunotherapy directed at TMGs has been challenging because of the low immunogenicity associated with glycolipids; that is, the carbohydrate part that constitutes the antigenic determinant of glycolipids is not adequately presented in the context of MHC/HLA [93].

To induce antibodies against gangliosides, it was first covalently linked to KLH (keyhole limpet hemocyanin) and combined with a saponin adjuvant [94]. Vaccination of melanoma patients with GM2-KLH conjugate vaccines resulted in a high titer antibody response in most patients. Applying this concept to GD2 and GD3, unfortunately, failed to induce a consistent antibody response. Thus, the conjugate was changed to GD2 lactone based on the observation that a GM3 lactone is a more effective immunogen than GM3 alone. However, using this approach to immunization against GD2 showed, at best, a short-lived induction of antibodies against GD2 [95]. As a last resort, the chemical conjugation of glycans to a protein scaffold to turn carbohydrates from T-cell-independent antigens to T-cell-dependent antigens was also tested [96]. This procedure, however, did not lead to any positive results.

It was also noted that all ganglioside vaccines induced a humoral response (testing serum for antibodies after vaccination) but failed to show a persistent immunity [89]. Ganglioside vaccines were originally thought to elicit antibodies following the antigen presentation through an alternative presentation pathway using the cluster of differentiation 1 (CD1) route [97]. In contrast to the classical antigen presentation pathway through the major histocompatibility complex (MHC) class I and II used by protein-derived antigens, glycolipids

are presented through the CD1 mediated alternative route. However, such antibody responses to gangliosides are only temporary [98], and there was no direct correlation between anti-ganglioside antibody titer and anti-tumor effect [89].

Recently, dendrimers of GD2 and GD3 were synthesized using a matching glycomimetic, which are chemical structures that mimic the organic function of carbohydrates. The glycomimetic precursors were then conjugated to a tetrameric polyamidoamine (PAMAM) to generate oligomers “PAMAM-GD2” and “PAMAM-GD3,” which are water-soluble, lipid-free, and maintain the original structure found in gangliosides [99].

In this proof-of-concept study, PAMAM-GD2 and PAMAM-GD3 used as vaccines seem to confer high immunogenicity and are able to elicit humoral responses that are selectively cross-reactive with GD2 or GD3 on the tumor cell surface [89]. Further studies are still underway to check the feasibility of combining immune-checkpoint inhibition with these vaccines.

The absence of long-lasting immunity following ganglioside vaccination is likely attributed to the use of alternative antigen presentation pathways by gangliosides mediated through CD1. This alternative pathway is not effective in the activation of effective CD4-T helper immune response (T-cell independence), as is the case following classical antigen presentation pathways of peptides through MHC class I and II, which is critical to induce long-lasting and persistent immunity. To overcome the obstacle of T-cell independency of glycolipids, peptide mimotopes were created to functionally mimic the nominal antigen.

Mimotopes

Mimotopes are peptides that mimic epitopes of carbohydrates that can be identified through phage display technology [100]. Phage display technology allows for the selection of mimotopes that are structurally similar to B cell epitopes [101]. Phage libraries express a large variety of octa- or nona-peptides with up to 10^7 different peptide sequences expressed on the surface of the phage. The peptide of choice can then be selected by repetitive biopanning procedures [102].

Based on this concept, GD2 mimotopes were identified through biopanning of a phage display library against the ch14.18 mAb [103]. First, two plasmid DNA minigene vaccines were produced that encoded for two GD2 mimotopes. The ability of these vaccines to induce a tumor protective immune response was then studied in the syngeneic immunocompetent NXS2 neuroblastoma mouse model expressing GD2. The results showed that mice receiving the mimotope vaccine had a 50% decrease in tumor growth with a concomitant decrease in liver metastases. Also, the highest anti-GD2 humoral immune response was observed in the sera of mice that received the vaccine [103, 104].

In an effort to further improve the specificity of the selected GD2 mimotope-peptide, systematic amino acid substitution analysis was done using SPOT (Synthetic Peptide Arrays on Membrane Supports) technology. SPOT is a method allowing the parallel synthesis of large numbers of peptides that differ in one amino acid at each position of the original peptide [105]. With this method, a peptide C3 with increased binding affinity to anti-GD2 antibodies was generated [106]. This optimization resulted in a further decrease in primary tumor growth and metastasis than the original peptide mimotope. C3-KLH vaccination was also associated with an anti-GD2 serum response favoring the creation of IgG subclass 1, which is usually seen as a humoral immune response following the classical T-cell dependent activation, in contrast to IgG2a, which is typically associated with a response against T-cell independent antigens.

Anti-Idiotype vaccines

Another important strategy to overcome the limitation of T-cell independency of glycolipid antigens lies in the use of anti-idiotypic mAbs (Figure 2), also known as Ab2, which function as surrogate antigens and, as such, have the capacity to regulate the host's immune response.

The utilization of Ab2 instead of antigens as vaccines has been studied [107], and is primarily based on Jerne's theory that the immune system is an integrated network consisting of antibodies and lymphocytes [108]. Using Jerne's postulate, immunization with an antigen leads to the formation of antibodies (Ab1) directed specifically against this antigen. Ab1 antibodies can then lead to the formation of anti-idiotypic antibodies (Ab2) aimed against these Ab1 antibodies. The ensuing Ab2 antibodies are then structural and functional mimics

of the original antigen and can therefore be used as immunogens to stimulate a specific immune response similar to those produced by the initial or nominal antigen [109, 110].

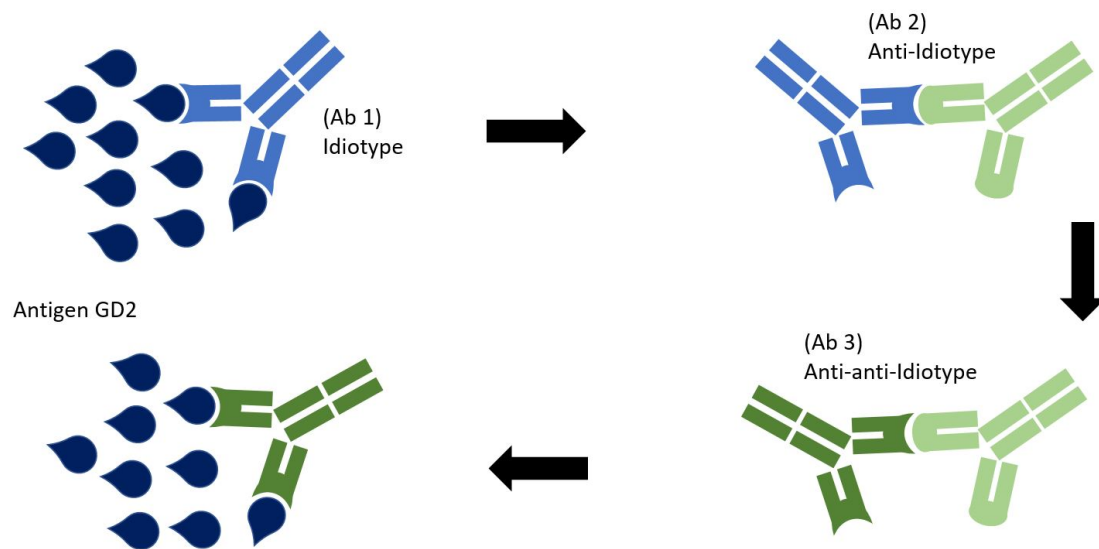


Figure 2. Jerne's network model of idiotypic interactions using GD2 as an example

The GD2 specific immunotherapy against neuroblastoma with dinutuximab-beta is equivalent to antibody (Ab1) in Jerne's network theory. The paratope of dinutuximab-beta which recognizes the antigen GD2 also has an immunogenic effect, thus creating an anti-idiotypic antibody (Ab2) which is a "photographic negative" of Ab1 and therefore mimics the original antigen GD2 structure. The Ab2 antibody consecutively leads to a further immune reaction, and the resulting antibodies (Ab3) can cross-react with the antigen GD2 due to the "molecular mimicry" between GD2 and anti-idiotypic (Ab2) thereby inducing a therapeutic effect.

Monoclonal Ab2, as a cancer vaccine, offers several advantages. One of which is its high specificity since it only mimics a single epitope of a tumor antigen. Another advantage is its ability to stimulate B cell clones [111] that tolerate the nominal antigen. Another feature is the absence of unwanted side effects (sometimes seen with standard antigen vaccines) due to the lack of dispensable components in the vaccine, such as tumor cells [112]. Finally, Ab2 vaccines are immunoglobulins that can be manufactured using standard and well-established techniques [112].

Anti-Id responses have been connected to the development of anti-tumor immunity to colorectal cancer. For example, clinical trials in human colorectal carcinoma patients with a polyclonal anti-Id against the mAb 17-1A (specific for Epithelial cell adhesion molecule; EpCAM) induced anti-tumor antibody responses [112]. Another similar study in melanoma

patients showed that intradermal injection of 2 mg of anti-Id mAb MK2-23 imitates the high-molecular-weight melanoma antigen (HMW-MAA) and evoked anti-tumor antibody responses [113]. A size reduction of metastatic lesions was consequently observed in 7 out of the 37 vaccinated patients.

In a second study, 25 patients with stage IV melanoma were immunized with the mouse anti-Id mAb MK2-23 of the anti-high-molecular-weight melanoma antigen (HMW-MAA) mAb 763.74, which is a mimic of an epitope of HMW-MAA. Fourteen patients developed antibodies against HMW-MAA (Ab3) as determined by immunochemical and serologic assays, and they were shown to identify the identical or a structurally close epitope as the anti-HMW-MAA mAb 763.74 (Ab1) [114].

Side effects consisted of induration, erythema, and ulceration at injection sites. Patients sometimes also complained of flu-like symptoms, myalgias, and arthralgias. Three patients who developed anti-HMW-MAA antibodies showed incomplete responses, consisting of a size reduction in the metastatic lesions that lasted 52 weeks in one patient and 93 weeks in the other two. Survival of the 14 patients with confirmed anti-HMW-MAA antibodies was significantly longer than that of the nine patients without a detectable anti-HMW-MAA response [112, 114].

These clinical observations show that anti-Id vaccines are a promising approach to generating tumor-specific immunity without inducing autoimmunity.

Ganglidiomab

A novel anti-GD2 anti-idiotypic antibody (ganglidiomab) was generated using the same concept described above and used as a vaccine against NB [3].

The generation of the anti-idiotypic antibody ganglidiomab was accomplished through the following steps. First, Balb/c mice were immunized with a monoclonal anti-GD2 antibody (14G2a) conjugated with ovalbumin. Anti-14G2a antibody titers in mouse sera were then analyzed using a sandwich ELISA. Splenocytes of mice developing anti-14G2a antibodies were then fused with SP2/0-Ag 14 cells and were later screened and cultivated as hybridoma cells. Finally, subcloning of hybridomas that have immunoglobulins binding to ch14.18 was performed through limiting dilution technique with 1–3 cells/well. To assess whether

immunoglobulins mimic the nominal antigen GD2 (i.e., anti-idiotypic properties), they were tested to inhibit the binding of anti-GD2 antibodies of the 14.18 family to GD2 antigen using ELISA. One hybridoma that secreted an immunoglobulin with the characteristics described above was then selected and named ganglidiomab.

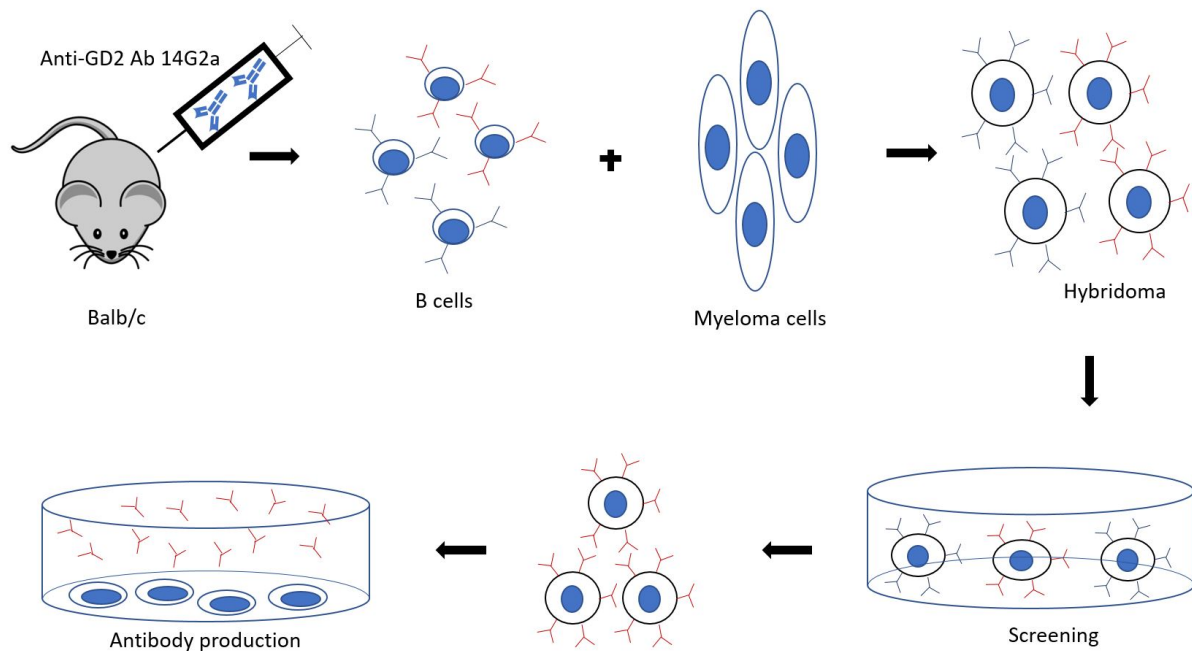


Figure 3. Generation of ganglidiomab through the use of classic hybridoma technology

Balb/c mice were immunized with murine anti-GD2 antibody 14G2a. The spleen of immunized mice containing primed B-cells were used to create hybridoma cells using murine non-secreting myeloma cells SP2/0 as a partner cell line. The hybridoma cells were subcloned, and clones were selected according to their ability to secrete anti-14G2a antibodies for further characterization.

After the immunization of Balb/c mice with the anti-GD2-Ab-14G2a, the spleens of the mice were used as a source of B-cells (1.) that were immortalized by fusion with the non-secreting myeloma cell line SP2/0. The resulting hybridoma cells (2.) were subcloned and tested for antibody production and specificity for the immunogen (i.e. 14G2a) (3.). Clones tested positive for an antibody binding to 14G2a were further examined whether they also mimic GD2. This was determined by the ability of such antibodies to inhibit ch14.18 binding to GD2 using an ELISA method [84]. After several rounds of subcloning, the ganglidiomab-producing hybridoma was then selected (4.) and further cultivated for antibody production (5.)

Since antibodies that bind to ch14.18 outside of the variable region are irrelevant, identifying the function of the secreted immunoglobulin from hybridoma clones as an anti-Id (or as a GD2 mimotope) was crucial. This was done through competitive ELISA, that is, only immunoglobulins secreted from hybridoma capable of competitively inhibiting the binding of ch14.18 to GD2 were selected. After several rounds of subcloning, a stable hybridoma was selected, and the produced immunoglobulin was referred to as ganglidiomab.

Ganglidiomab was further characterized structurally and functionally, and its variable (VL and VH) regions were subsequently cloned and sequenced [3].

In a preclinical study, mice were either immunized with ganglidiomab or in combination with an adjuvant, and the corresponding humoral response was determined through GD2 ELISA [3]. Mice vaccinated with ganglidiomab showed a humoral anti-GD2 immune response *in vivo* compared to the control group receiving adjuvant alone. More importantly, the ELISA signals also showed complete blocking when sera of immunized mice were treated with a surplus of ganglidiomab, thereby proving the specificity of the humoral immune response for GD2 [3]. To determine the anti-neuroblastoma activity of the vaccine, ADCC and CDC assays from sera of immunized mice and their controls were tested. Results showed that only sera of mice vaccinated with ganglidiomab was able to elicit a cytotoxic activity against neuroblastoma target cells in both assays, solidifying the functional anti-neuroblastoma activity following vaccination with ganglidiomab.

2. Objectives

Here, we investigated the immune response of a ganglidiomab vaccine in seven patients with high-risk neuroblastoma in a compassionate use program. We hypothesized that high-risk neuroblastoma patients who completed standard multimodal high-intensity treatment, including high-dose chemotherapy followed by autologous stem cell transplantation and passive immunotherapy with dinutuximab-beta, who then receive vaccination with an anti-idiotypic antibody of dinutuximab-beta, will develop an endogenous anti-GD2-antibody response. We also evaluated the outcome compared to historical controls.

3. Methods and patients

3.1. Preparation of the vaccine

Ganglidiomab antibody produced through the hybridoma technology (see Figure 3) was diluted to a final concentration of 1mg/ml following this protocol:

3.5 ml	ganglidiomab (10mg/ml, corresponding to 35mg ganglidiomab)
27.603 ml	NaCl phys.
3.8987 ml	Alhydrogel (116.91mg corresponding to 3.34mg/ml in the final suspension)
35 ml	final suspension (final concentration of ganglidiomab – 1mg/ml)

0.6 ml aliquots of the final suspension were filled into glass vials under sterile conditions and sealed.

3.2. Vaccination schedule

Ganglidiomab was administered subcutaneously every two weeks using a dosage of 0.5mg (0.5ml) with 1.67mg aluminum as adjuvant. The median interval between initial diagnosis and first vaccine dose was 29 months (range 18-40 months), and all patients received at least six injections (median 7, range 6-22) (see Table 3).

Table 3. Time from initial diagnosis to start of vaccination and number of ganglidiomab doses

Patient	Interval ¹	Number of doses received ²
IA	29 months: 10/2010 – 11/2012	8
MN	40 months: 01/2010 – 05/2013	22
SL	34 months: 05/2011 – 03/2014	12
SA	33 months: 02/2012 – 11/2014	7
ST	22 months: 01/2013 – 11/2014	7
PM	18 months: 05/2013 – 11/2014	6
MA	29 months: 06/2012 – 11/2014	6

¹ Number of months from the initial diagnosis of neuroblastoma to the first dose of ganglidiomab given to each patient. The median interval is 29 months (range 18-40 months).

² Number of doses received: median 7, range 6-22.

3.3. Patient characteristics

Table 4. Patient characteristics enrolled in the compassionate use program

Patient	Age at Diagnosis	Sex	Height	Weight	BSA ¹	Stage	N-myc amplification ²
IA	3 years	M	129,5cm	23kg	0.9m ²	4	no
MN	25 years	F	166cm	48.7kg	1.50m ²	4	no
SL	1 month	M	88cm	14.1kg	0.59m ²	4 (initial 2/3)	yes (initial no)
SA	3 years	F	97cm	14.85kg	0.63m ²	4	unknown
ST	6 months	M	81cm	11kg	0.50m ²	4	yes
PM	7 years	F	131.5cm	36.2kg	1.15m ²	4	yes
MA	5 years	M	117cm	18kg	0.76m ²	4	yes

¹ BSA – Body Surface Area is equal to the square root of the product of the weight (kg) multiplied by the height (cm) divided by 3600, expressed in square meters (m²).

² N-myc gene is a proto-oncogene protein whose amplification signifies a crucial prognostic factor in neuroblastoma associated with poor prognosis and unfavorable outcome.

During the period from March 2013 to November 2014, 7 patients with stage 4 NB who previously received anti-GD2 immunotherapy with dinutuximab-beta at our institute were enrolled in this program. The median age at diagnosis was at three years (range - one month to 25 years), with 3 of the subjects being females and the rest males. Table 4 also lists the presence of n-myc amplification among the included patients, with 4 out of the 7 subjects having n-myc gene amplification. SL, who was diagnosed with localized neuroblastoma (stage 2/3) at the age of one month, did not initially show n-myc amplification. However, in the course of his treatment, a metastatic relapse and progression to stage 4 were diagnosed with a concomitant switch to n-myc amplification, changing the patient's status from low-risk to high-risk, eventually requiring intensification of his treatment. Patient MN, on the other hand, died due to an anaphylactic reaction not related to neuroblastoma.

Table 5. Patients' medical history and comorbidities

Patient	
IA	NA ¹

MN	Secondary hypothyroidism, VRE ² (E.facium) and ESBL ³ (Klebsiella, E.coli) carrier, ambisome allergy, chronic iritis OU, herpes zoster, renal failure with salt wasting, squamous cell carcinoma of the upper esophagus as second primary cancer
SL	Gait disorder, scoliosis, ASD II ⁴ , incomplete horner's syndrome (right)
SA	Gentamicin allergy, right distal fibula fracture
ST	Ifosfamid intolerance, ESBL ³ carrier (E.Coli) in stool
PM	Focal nodular hyperplasia, ESBL ³ carrier in stool, mild high frequency hearing loss
MA	Hypothyroidism, high frequency hearing loss, recurrent catheter-related infection with S.epidermidis

¹ NA – not applicable

² VRE – Vancomycin Resistant Enterococcus and

³ ESBL – Extended Spectrum Beta-Lactamase, are multidrug-resistant organisms that commonly occur among immunodeficient persons and can be sources of infection for the carrier.

⁴ ASD – Atrial Septum Defect is a congenital heart defect characterized by a persistent hole between the two atria.

The above table lists the previous medical histories of the subjects and their active comorbidities. Of note is the development of a secondary cancer in MN after completing the therapy for NB. Furthermore, most of the listed comorbidities are chemotherapy-related long-term complications that occur shortly after the end of treatment (i.e., hearing loss, hypothyroidism, infections).

Table 6. Treatment received from initial diagnosis

Patient	Induction	Consolidation	Maintenance	Relapse/Progression
IA	Rapid COJEC ¹ , surgery of primary lesion	BuMeI ² /ASCT ³ , radiotherapy	dinutuximab beta/IL-2 ⁴	No
MN	NB 2004 HR	BuMeI ² /ASCT ³ , MIBG ⁵ (stem cell boost)	dinutuximab beta/IL-2 ⁴	Yes. Transarterial chemoembolization (TACE ⁶), MIBG ⁵ right hemihepatectomy with laser coagulation of new herds in the liver, RIST ⁷ , MIBG ⁵ , haploidentical SCT, dinutuximab beta/IL-2 ⁴

SL	Tumor biopsy, right adrenalectomy with lymphadenectomy, NB 2004 HR	MEC ⁸ /ASCT ³	Isotretinoin ¹⁰ , dinutuximab beta/IL-2 ⁴	No
SA	NB 2004, surgical resection of primary tumor and retroperitoneal lymph nodes	MEC ⁸ /ASCT ³	Isotretinoin ⁹ , dinutuximab beta/IL-2 ⁴	Yes. Relapse treatment – RIST ⁷ , stem cell apheresis ¹⁰ , MIBG ⁵ therapy + Topotecan ¹¹ , re-transfusion of autologous stem cells, dinutuximab beta/IL-2 ⁴ , radiotherapy of the left proximal femur (30Gy)
ST	SIOPEN 2001/GPOH ¹² (initial diagnosis of neuroblastoma), tumor biopsy, NB 2004 HR, left adrenalectomy	MEC ⁸ /ASCT ³	Isotretinoin ⁹ , dinutuximab beta/IL-2 ⁴	No
PM	NB 2004 HR [115], Topotecan, Cyclophosphamide	MIBG ⁵ , BuMel ² /ASCT ³	Isotretinoin ⁹ , dinutuximab beta/IL-2 ⁴	No
MA	Tumor resection with left adrenalectomy, NB 2004 HR, Chemotherapy (Cyclophosphamide, Doxorubicin, Vincristine, Cisplatin, Etoposide) in Korea	BuMel ² /TBI ¹³ (10Gy), ASCT ³ , MIBG ⁵	Isotretinoin ⁹ , Thalidomide ¹⁴ , dinutuximab beta/IL-2 ⁴	No

¹ COJEC – Cisplatin, Vincristine, Carboplatin, Etoposide and Cyclophosphamide (cisplatin is represented by the first C of the acronym, otherwise abbreviated (P), vincristine (O), carboplatin (J), etoposide (E), and cyclophosphamide (C) is the high-dose rapid and standard induction chemotherapy program for patients with stage 4 neuroblastoma.

² Bu/Mel – Busulfan and Melphalan is the European standard high-dose chemotherapy for HR-NB.

³ ASCT – Autologous Stem Cell Transplant is a treatment modality used for solid tumors to bridge hematopoietic failure during high-dose chemotherapy. In this procedure, stem cells are collected from the patient, stored, and reinfused back to the patient after chemotherapy and/or radiation. In contrast, a haploidentical Stem Cell Transplant (haplo SCT) is a type of allogeneic transplant where healthy stem cells from a half-matched donor are collected and given to the patient.

- ⁴ IL-2 – Interleukin-2 is a cytokine released by T cells in response to an antigen, which regulates the proliferation and differentiation of natural killer cells, B cells and other T cells.
- ⁵ MIBG – Metaiodobenzylguanidine is a guanithidine analog used for imaging and therapy of neuroblastomas and various neural crest tumors.
- ⁶ TACE – Transarterial Chemoembolization is a non-surgical, minimally invasive procedure that combines the local delivery of chemotherapy with embolization to treat cancer.
- ⁷ RIST – Rapamycin, Irinotecan, Dasatinib, and Temozolomide is a treatment regimen used for patients with relapsed or progressive HR-NB.
- ⁸ MEC – Melphalan, Etoposide, and Carboplatin is the current US standard for high-dose chemotherapy before stem cell rescue for HR-NB.
- ⁹ Isotretinoin or 13-cis-retinoic acid (13-cis-RA) is a derivative of Vitamin A that can cause the arrest of cell growth and differentiation of neuroblastoma cell lines, thereby improving EFS in HR-NB.
- ¹⁰ Stem cell apheresis is the process of collecting stem cells from the peripheral blood as part of stem cell transplantation.
- ¹¹ Topotecan is a Topoisomerase I Inhibitor that inhibits the topoisomerase I enzyme in replicating cells leading to the induction of DNA single and double strand breaks resulting in cell death.
- ¹² GPOH – Gesellschaft für Pädiatrische Onkologie und Hämatologie or Society for Pediatric Oncologists and Hematologists
- ¹³ TBI – Total Body Irradiation is a form of radiotherapy used primarily as part of the preparatory phase before a hematopoietic stem cell transplantation.
- ¹⁴ Thalidomide is an anti-angiogenic agent that causes suppression of blood vessel proliferation.

The current therapy for neuroblastoma is divided into three phases—induction, consolidation, and maintenance therapy. As seen above, treatment includes chemotherapy, surgical resection, high-dose chemotherapy with autologous stem cell rescue, radiation therapy, immunotherapy, and isotretinoin [116]. The induction regimens for high-risk neuroblastoma can vary depending on where a patient is being treated. During induction, patients usually receive 6–8 cycles of intensive chemotherapy, including platinum, alkylating, and topoisomerase agents. Some induction regimens also include vincristine, doxorubicin, cyclophosphamide, cisplatin, and etoposide [116]. Also, the COG trials have added topotecan during the first two cycles of induction. Six of the seven patients listed in the above table were treated according to the NB 2004 HR protocol. In contrast, patient IA was treated according to the Society of Pediatric Oncology Europe Neuroblastoma Group (SIOPEN) regimen (rapid COJEC) that gives repeated cycles with a shortened recovery interval which led to fourteen-day cycles [65]. This regimen utilized combinations of vincristine, carboplatin, etoposide, cyclophosphamide, and cisplatin in a total of eight cycles.

Surgery is another main component of HR-NB therapy and typically occurs at or near the end of induction chemotherapy. Except for MP and MN, all of the patients underwent resection of

their primary tumor. In the case of MN, surgery was only performed during her relapse treatment.

The consolidation phase, which follows induction, is divided into two parts and includes high-dose chemotherapy followed by autologous stem cell transplant (ASCT) with or without radiation therapy [116]. All seven patients underwent stem cell collection in preparation for their ASCT. In addition, MA and IA further underwent radiotherapy of their primary residual tumors.

Conditioning regimens for ASCT in patients with HR-NB have conventionally differed between North America and Europe. The COG had typically utilized MEC (melphalan, etoposide, and carboplatin) while the Europeans used Bu/Mel (busulfan/melphalan). Three of the seven patients (SA, ST, and SL) received the conditioning therapy according to the COG regimen, and the rest of the subjects followed the Bu/Mel protocol.

The post-consolidation or maintenance phase of therapy was intended to treat the remaining residual disease despite intensive induction and consolidation treatment [116]. All patients in this study received immunotherapy with an anti-ganglioside GD2 antibody (dinutuximab-beta) in combination with the cytokine IL-2, with five of them further receiving isotretinoin (PM, SA, MA, ST, and SL) as part of their treatment.

Two of the seven patients (SA and MN) additionally underwent relapse treatment at the end of their maintenance therapy. This treatment included undergoing the RIST protocol [117], another round of MIBG, ASCT, immunotherapy with dinutuximab-beta, and radiotherapy. For MN, surgery was also done to remove liver metastases. In contrast to SA, MN received a haploidentical SCT after receiving conditioning chemotherapy with fludarabine, thiotepa, melphalan, and ATG as part of her relapse treatment, followed by dinutuximab-beta [118].

3.4. Side effects of the vaccine

Side effects following the injection of the ganglidiomab vaccine were recorded in the patient's charts. Only local injection reactions with transient erythema of a maximum duration of 48

hours were noted, which were Grade 1-2 according to the Common Terminology Criteria for Adverse Events (CTCAE). There was no fever or any other systemic side effect recorded.

3.5. Determination of immune response

The immune response of immunized patients was determined against three different antigens using Enzyme-linked Immunosorbent Assays (ELISA). The first ELISA determined whether the patient is developing a response against ganglidiomab (murine IgG) used for vaccination. The second assessment involved an ELISA analysis of the patient's response against the variable region of ganglidiomab (Fab), which contains the GD2 mimotope. For this purpose, a human-mouse chimeric version of ganglidiomab (ganglidiximab, of which the Fab region is murine, and the constant regions are human) was used since the response against the Fab (and not the constant regions) was the desired outcome of the vaccination with ganglidiomab. Finally, the third ELISA analysis included determining the patient's response against the ganglioside GD2, which was the ultimate goal following vaccination with ganglidiomab.

3.5.1. Binding of antibodies from serum of immunized patients to ganglidiomab

The antibody response against the ganglidiomab vaccine in serum of immunized patients was performed as previously described [119] using ELISA with some modifications. In brief, 96-well immunoplates (PAA, Pasching, Austria) were coated with 250ng per well ganglidiomab (100µl per well; 0.1 M carbonate/hydrogen carbonate buffer, pH 9.6, 1 h 37°C). After undergoing three wash steps with PBS (phosphate-buffered saline) (pH 7.4; PAA, Pasching, Austria) supplemented with 0.1% (v/v) Tween-20 (Applichem, Darmstadt, Germany), the wells were blocked with 1% (w/v) BSA (bovine serum albumin) (200µl per well; Sigma Aldrich, Steinheim, Germany) in PBS (1h, 37°C) and washed again three times (200µl per well; 0.1% BSA in PBS, pH 7.4). The patient's serum was then diluted 1:800 in PBS and incubated overnight (100µl per well; +4°C). The antibodies that were bound to ganglidiomab were detected after five wash steps (200µl per well; 0.1% Tween-20 in PBS, pH 7.4) with 100µl per well horseradish peroxidase (HRP)-conjugated goat anti-human IgG antibody used as a secondary antibody (1/20,000, 1h, 37°C; Sigma Aldrich, Steinheim, Germany).

Plates were washed with 0.1% BSA in PBS (5x), followed by the addition of 75µl per well 3,3',5,5'-tetramethylbenzidine (TMB) substrate reagent following the manufacturer's guidelines (R&D Systems Inc., Minneapolis, MN, USA). The reaction was terminated by the addition of 2 N H₂SO₄ (50µl) after 30 min. Absorption was analyzed at 450nm in a plate reader (BioTek Instruments, GmbH, Bad Friedrichshall, Germany). Naive patients serum were also diluted in 1:800 PBS (100µl per well; Polymun Scientific, Vienna, Austria), and murine IgG1 as a capture Ab (100µl per well; carbonate/hydrogen carbonate buffer R&D Systems Inc., Minneapolis, MN, USA) were used as negative controls for ganglidiomab-based ELISA.

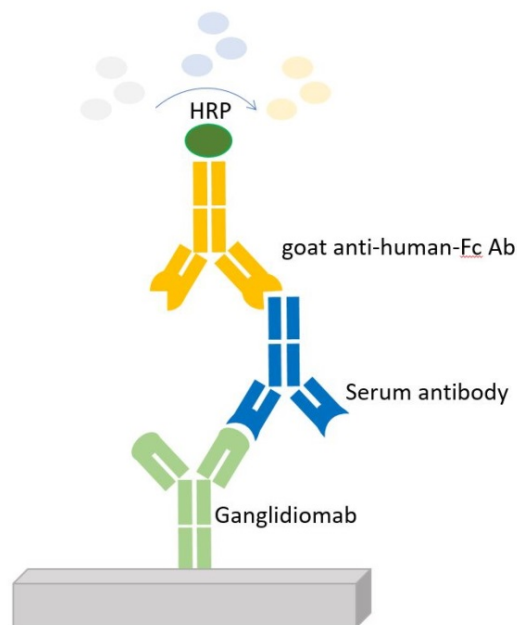


Figure 4. Schematic for the detection of an anti-ganglidiomab immune response in the serum of immunized patients

The serum of immunized patients is dispensed into ganglidiomab coated microwell plates and washed. A horseradish peroxidase (HRP)-enzyme-labeled secondary antibody (goat anti-human Fc Ab) is added. A second wash step removes the unbound secondary antibody. The signal is generated through the addition of 3,3',5,5'-tetramethylbenzidine (TMB) substrate leading to an enzymatic color change from colorless to blue (through HRP) that is transformed into yellow after addition of the sulfuric acid (stop reagent).

3.5.2. Binding of antibodies from the serum of immunized patients to ganglidiomab

Ganglidiomab is a human mouse chimeric version of ganglidiomab and was engineered as previously described [120].

Preparation of biotinylated ganglidiomab used as a detection antibody

The production of biotinylated ganglidiomab was done using 1 mg/ml of ganglidiomab mixed with 1× PBS (Capricorn Scientific GmbH, Ebsdorfergrund, Germany, Cat. PBS-1A) incubated for 30 min at RT with 10 mM biotin (EZ-Link® Sulfo-NHS-LC-Biotin; Thermo Scientific, Erlangen, Germany) diluted in distilled water according to the manufacturer's guidelines. Unbound biotin was removed by dialysis with PBS (pH 7.4) overnight at RT using a regenerated cellulose dialysis membrane (molecular weight cut-off (MWCO) 12,000–14,000; pore diameter 25 Å; VISKING® Dialysis Tubing, Serva Electrophoresis GmbH, Heidelberg, Germany). Aliquots of biotinylated ganglidiomab were then stored at +4 °C.

ELISA procedure for the detection of a response against ganglidiximab

Anti-ganglidiximab response in serum of NB patients was detected through an ELISA method using ganglidiximab as a capture Ab and biotinylated ganglidiomab as a detection Ab following the one-arm binding principle (Figure 5). Here, the anti-GD2 antibody ch14.18/CHO was used as a standard and quality control (QC).

96-well immunoplates (Sarstedt, Nümbrecht, Germany, Cat. 82.1581.200) were coated with 250 ng of ganglidiximab per well (100 µl/well) prepared in 15 mM sodium carbonate coating buffer (pH 9.6) and incubated for 1 h at 37 °C. After washing (3×; 0.1% Tween-20 in PBS) and blocking with 1% BSA in PBS (pH 7.4; 1 h, 37 °C) standard samples containing dinutuximab-beta (ch14.18/CHO) in human serum were prepared by 1:2 serial dilutions to yield 25.0, 12.5, 6.25, 3.13, 1.56 and 0.78 µg/ final concentrations. Thereafter, the standard and patient samples were diluted 1:160 using 1× PBS (pH 7.4), and 100 µl/well were incubated overnight at 4 °C.

Thereafter, plates were washed five times, and biotinylated ganglidiomab (2 mg/ml; 1:2,500) was added as a detection Ab for 2 h at 37 °C followed by three wash steps. To detect binding of biotinylated ganglidiomab to anti-ganglidiximab antibody (patient sample) or ch14.18/CHO (standard) bound to ganglidiximab capture Ab, a high sensitivity NeutrAvidin-HRP conjugate was used (1:10,000 in 1% (w/v) BSA in PBS (pH 7.4), 20 min, 37 °C; Thermo Scientific, Erlangen, Germany, Cat. 31030). Plates were then washed five times, a substrate reagent TMB was added for 12 min (RT, dark), and the reaction was stopped by the addition of 2 N H₂SO₄ (50

$\mu\text{l/well}$). Finally, absorption was determined in the plate reader (BioTek Instruments GmbH, Bad Friedrichshall, Germany) at 450 nm.

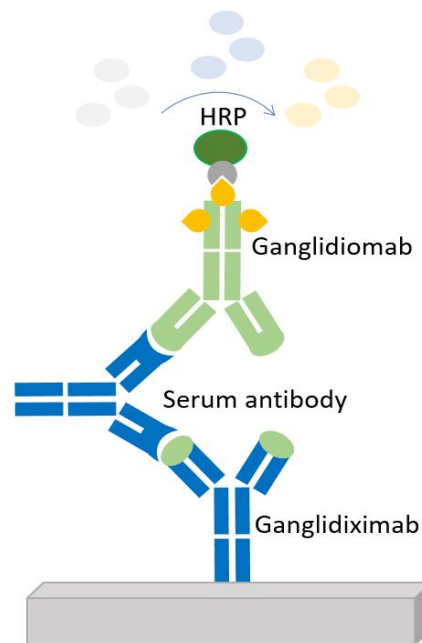


Figure 5. Schematic for the detection of an anti-ganglidiximab response in the serum of immunized patients (one-arm principle)

The serum of immunized patients is dispensed into microwell plates coated with ganglidiximab, and washed. An enzyme-labeled secondary antibody (biotinylated ganglidiomab) is added for detection. A second wash step removes the unbound secondary antibody. The signal is generated as described in Figure 4.

3.5.3. Binding of antibodies from the serum of immunized patients to GD2

The antibody response of immunized patients against the antigen GD2 was investigated using ELISA as previously described [3]. In brief, 96-well immunoplates (PAA, Pasching, Austria) were coated with 50 ng per well GD2. After undergoing three wash steps with PBS (pH 7.4; PAA, Pasching, Austria) enhanced with 0.1% (v/v) Tween-20 (Applichem, Darmstadt, Germany), the wells were blocked with 1% (w/v) BSA (200 μl per well; Sigma Aldrich, Steinheim, Germany) in PBS (1h, 37°C) and washed again three times (200 μl per well; 0.1% BSA in PBS, pH 7.4). For quantification, a ch14.18/CHO standard curve was used. Ch14.18/CHO was then diluted 1:800

in PBS to final concentrations of 1.0, 0.5, 0.25, 0.13, 0.06, 0.03 and 0.015 $\mu\text{g}/\text{ml}$ and incubated overnight (100 μl per well; +4 $^{\circ}\text{C}$). Ch14.18/CHO bound to GD2 was detected after five wash steps (200 μl per well; 0.1% Tween-20 in PBS, pH 7.4) with 100 μl per well horseradish peroxidase (HRP)-conjugated goat anti-human IgG antibody used as a secondary antibody (1/20,000, 1h, 37 $^{\circ}\text{C}$; Sigma Aldrich, Steinheim, Germany).

Plates were washed with 0.1% BSA in PBS (5x), followed by the addition of 75 μl per well 3,3',5,5'-tetramethylbenzidine (TMB) substrate reagent following the manufacturer's guidelines (R&D Systems Inc., Minneapolis, MN, USA). The reaction was terminated by the addition of 2 N H_2SO_4 (50 μl) after 30 min. Absorption was analyzed at 450nm in a plate reader (BioTek Instruments, GmbH, Bad Friedrichshall, Germany). GM2 and GD1b 50ng per well (50 μl per well, 100% methanol; Sigma Aldrich, Steinheim, Germany) were used as negative controls for GD2-based ELISA. To show competitive inhibition of the antibodies from serum of immunized patients binding to GD2, samples were pre-incubated with an excess of ganglidiomab (70 $\mu\text{g}/\text{ml}$) for 20 min at room temperature (RT).

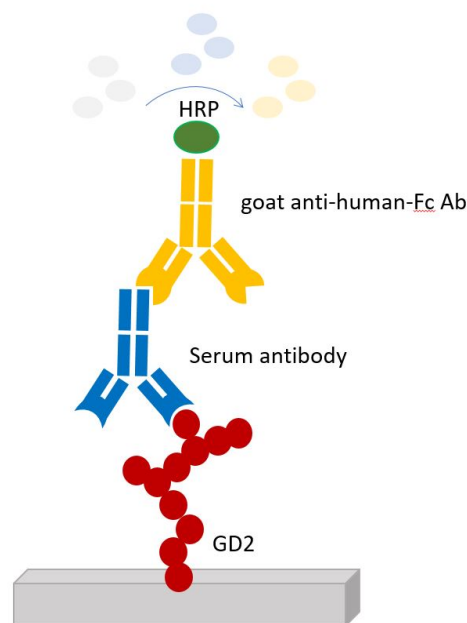


Figure 6. Schematic for the detection of an anti-GD2 response in the serum of immunized patients

The serum of immunized patients is dispensed into microwell plates coated with GD2 and washed. An HRP-labeled secondary antibody (goat anti-human Fc Ab-HRP) is added and allowed to attach to the serum antibody. After a second wash step the signal is generated as described in Fig. 4.

3.5.4. Determination of complement dependent cytotoxicity of immunized patients

The GD2 specific complement-dependent cytotoxicity of immunized patients against neuroblastoma cells in vitro was determined and described in the paper by Siebert, N., et al [121]. Here, the optimal dilution factor was ascertained through serial dilution of serum of healthy donors as complement source to study the impact of different serum concentrations on CDC activity. First, nine serum concentrations were analyzed: 100%, 50%, 25%, 12.5%, 6.2%, 3.1%, 1.6%, 0.8% and 0.4%. Calcein-AM (acetomethoxy derivate of calcein) marked 0.6×10^6 LA-N-1 cells (human GD2-positive NB cell line) [121] underwent an incubation period of four hours (37°C, dark) with two defined concentrations of anti-GD2 mAb ch14.18/CHO (1.0 and 0.1 µg/ml), which were produced using the serum of a healthy donor.

Furthermore, to prove CDC specificity of the target cell lysis, a humanized mAb eculizumab (trade name Soliris; Alexion Europe SAS, Paris, France), known to selectively inhibit the splitting of complement protein C5 to C5a and C5b by the C5 convertase, was used.

The optimum GD2-specific CDC of NB cells LA-N-1 was found to be induced when utilizing 1.0 µg/ml ch14.18 prepared in a healthy donor serum with a 12.5% end concentration. To prevent ch14.18-mediated CDC, samples were pre-incubated with 1:10 serial dilutions of 1.0 mg/ml eculizumab prepared in 1x PBS (final concentration: 1000, 100, 10, 1, 0.1 and 0.01 µg/ml). Samples pre-incubated with an excess of the anti-idiotypic (anti-Id) Ab ganglidiomab (5.0 µg/ml) were included to prove GD2-specific target cell lysis. As negative control, rituximab (1.0 µg/ml) was used.

To evaluate CDC effector functions following vaccination with ganglidiomab, serum of immunized patients, collected on the same day of vaccination, were analyzed. Cytotoxicity was determined using a calcein-acetoxymethyl ester (AM)-based cytotoxicity assay as previously described [121]. To check for CDC, serum without effector cells (12.5% final concentration) was incubated with 5,000 calcein-AM-tagged LA-N-1 cells for 4 hours. Afterwhich, supernatants of each well were transferred to black 96-well plates to determine fluorescence at 495 nm excitation and 515 nm emission wavelengths employing a multimode microplate reader. Patient samples including specimens for spontaneous (target cells only)

and maximum release (target cells disrupted using an ultrasonic homogenizer), were examined at least six times. Cytotoxicity in percent mediated by ADCC was measured using the formula: $(\text{experimental release} - \text{spontaneous release}) / (\text{maximum release} - \text{spontaneous release}) \times 100\%$. For CDC, the cytotoxicity was calculated according to the formula: $(\text{experimental release} - \text{negative control release}) / (\text{maximum release} - \text{negative control release}) \times 100\%$ [76].

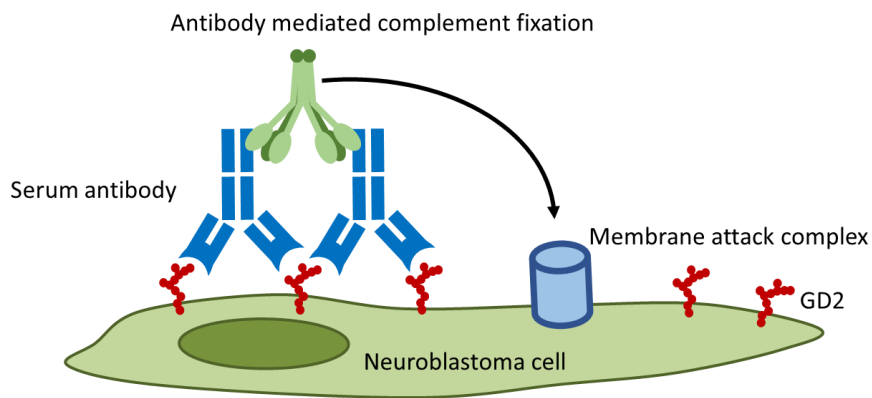


Figure 7. Complement dependent cytotoxicity in neuroblastoma

In this figure, the antibody-coated neuroblastoma cell recruits and activates components of the complement cascade, eventually leading to the formation of a membrane attack complex (MAC) on the cell's surface resulting in cell lysis.

4. Results

4.1. Analysis of raw data of patient SL as an example

Patient LS had a serum sample taken before receiving the first ganglidiomab vaccine to serve as baseline values. He was then immunized every two weeks starting 25/03/2014 and received a total of 10 doses.

For the immunomonitoring of patient SL, serum samples were taken on days 14, 28, 42, 56, 70, 84, 98, 112, 126, 140, and 154.

4.1.1. Anti-ganglidiomab immune response of SL

To quantify the anti-ganglidiomab immune response, a standard curve using known concentrations of 25.0 µg/ml, 12.5 µg/ml, 6.25 µg/ml, 3.1 µg/ml, 1.6 µg/ml, 0.8 µg/ml, and 0.0 µg/ml ch14.18/CHO was used in the ganglidiomab ELISA (schematic see Figure 4). The optical density signals at 450 nm obtained in the ELISA using these known concentrations were used to generate a standard curve (Table 7). All samples were analyzed in quadruplicates, and the standard deviation was calculated from 4 values per ch14.18 concentration.

Table 7. Optical density signals of varying ch14.18/CHO concentrations in the ganglidiomab ELISA.

Known ch14.18/CHO concentrations were used to create a standard curve in the ganglidiomab ELISA (schematic see Figure 4).

Standard (OD ¹ at 450nm)		
µg/ml	MEAN ²	SD ³
25.0	0.49	0.03
12.5	0.27	0.00
6.25	0.14	0.01
3.13	0.09	0.01
1.56	0.04	0.01
0.78	0.02	0.01
0.00	0.02	0.01
blank	0.00	0.01

¹ OD – Optical Density is the colorimetric change observed in this ganglidiomab assay, referring to the absorbance log at the chosen wavelength. The optical density is thus proportional to the amount of captured antigen in the sample. Results are expressed as Optical Density (**OD450**) measurements using a microplate reader with a 450nm filter.

² Mean, also known as average or arithmetic average or the sum of the values divided by the number of values.

³ SD – Standard Deviation measures the amount of variation or dispersion of a set of values. A low standard deviation indicates that the values are close to the mean of the group, while a high standard of deviation suggests that the values are spread out over a broader range.

With these values a standard curve was plotted using simple linear regression.

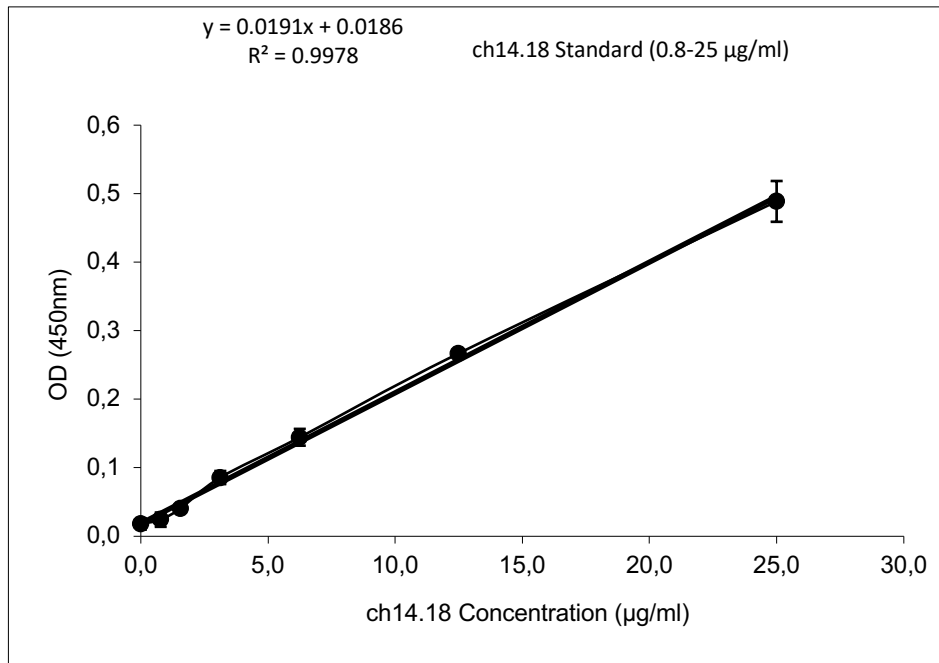


Figure 8. Standard curve representing the detectable concentration range for the detection of an anti-ganglidiomab response

The standard curve above represents the mean absorbance (here, the optical density) of the target protein (anti-ganglidiomab – y-axis) against a standard protein concentration. A best fit curve through the points in the graph is also drawn. Each point on the graph represents the mean of the four parallel titrations and its corresponding SD. A sample of known concentration (ch14.18 concentration – x-axis) is used as a positive control.

The simple linear regression model yields an equation of a linear curve, in this case $y = 0.0191x + 0.0186$, where y is the OD at 450 nm and x is the concentration in $\mu\text{g/ml}$. The regression coefficient R^2 indicates the fit of the values into the regression model and is generally acceptable for values >0.6 .

This equation is transformed to $x = (y - 0.0186) / 0.0191$ in order to calculate a concentration from the OD value obtained from the analysis of the serum of the immunized patient.

Table 8. Optical density signals in the ganglidiomab ELISA of serum taken at vaccination time points of patient SL analyzed in quadruplicates

Time Point	OD 450 values ¹			
baseline	0.00	0.00	-0.02	-0.01
14	0.40	0.39	0.40	0.39
28	0.91	0.92	0.92	0.90
42	0.92	0.92	0.92	0.91

56	0.96	0.97	0.95	0.97
70	1.08	1.09	1.08	1.10
84	1.09	1.12	1.11	1.13
98	1.15	1.11	1.12	1.16
112	1.19	1.20	1.17	1.37
126	1.16	1.39	1.17	1.17
140	1.13	1.14	1.15	1.13
154	1.19	1.19	1.20	1.18

¹ Optical density (OD) signals obtained from Day 0 until Day 154 and its corresponding values in quadruplicates determined using a plate reader (Synergy) HT at 450nm. The highlighted data are outliers and were excluded from further analysis using the outlier test according to Grubbs [122].

These OD data were used to calculate the concentration using the formula $x = (y - 0.0186) / 0.0191$

Table 9. Concentration of the anti-ganglidiomab response in the serum taken at vaccination time points of patient SL analyzed in quadruplicates

Time Point ¹	Concentration (µg/ml) ²				Mean ³	SD ⁴	SEM ⁵
baseline	0.14	0.25	-0.43	0.04	0.00	0.30	0.15
14	21.37	20.90	21.47	20.74	21.12	0.36	0.18
28	48.10	48.41	48.52	47.47	48.12	0.47	0.24
42	48.52	48.73	48.73	48.31	48.57	0.20	0.10
56	50.67	51.19	50.19	51.40	50.86	0.54	0.27
70	56.80	57.37	57.06	57.85	57.27	0.45	0.23
84	57.48	58.84	58.74	59.37	58.61	0.80	0.40
98	60.41	58.42	59.05	61.04	59.73	1.21	0.60
112	62.98	63.24	61.57		62.60	0.90	0.52
126	61.30		61.88	61.62	61.60	0.29	0.17
140	59.84	60.26	60.83	59.52	60.11	0.57	0.28
154	62.67	62.72	63.45	62.41	62.81	0.45	0.22

¹ Timepoint refers to vaccination days where serum samples were collected at 2-week intervals.

² Concentration refers to the antibody titer developed against ganglidiomab at different time points (baseline to Day 154) and in various measurements.

³ Mean, also known as average or arithmetic average or the sum of the values divided by the number of values.

⁴ SD – Standard Deviation measures the amount of variation or dispersion of a set of values.

⁵ SEM – Standard Error of the Mean represents the spread of the mean of a sample of values. SEM gives a more accurate representation of the mean, while SD gives an idea of the variability of the observations.

The highlighted data are outliers and were excluded from further analysis using the outlier test according to Grubbs [122].

The mean and standard error of mean were used to plot the curve of anti-ganglidiomab immune response as shown for all patients in Figure 11.

4.1.2. Anti-ganglidiximab immune response of SL

Similar to the quantification of the anti-ganglidiomab immune response, the anti-ganglidiximab response was also measured using the previously described standard curve with ch14.18/CHO concentrations in the x-axis and its corresponding optical density signals in the y-axis. Again, all samples were analyzed in quadruplicates, and the standard deviation was calculated from 4 values per ch14.18 concentration.

Table 10. Optical density signals of varying ch14.18/CHO concentrations in the ganglidiximab ELISA

Known ch14.18/CHO concentrations were used to create a standard curve in the ganglidiximab ELISA (schematic see Figure 5).

Standard (OD ¹ at 450nm)		
µg/ml	MEAN ²	SD ³
25.0	0.26	0.01
12.5	0.23	0.01
6.25	0.21	0.03
3.13	0.12	0.00
1.56	0.04	0.00
0.78	0.01	0.00
0.00	-0.01	0.00
blank	0.00	0.00

¹ OD – Optical Density is the colorimetric change observed in this ganglidiximab assay, referring to the absorbance log at the chosen wavelength. The optical density is thus proportional to the amount of captured antigen in the sample. Results are expressed as Optical Density (**OD450**) measurements using a microplate reader with a 450nm filter.

² Mean also known as average or arithmetic average or the sum of the values divided by the number of values.

³ SD – Standard Deviation measures the amount of variation or dispersion of a set of values.

A standard curve was then produced from the above values using linear regression.

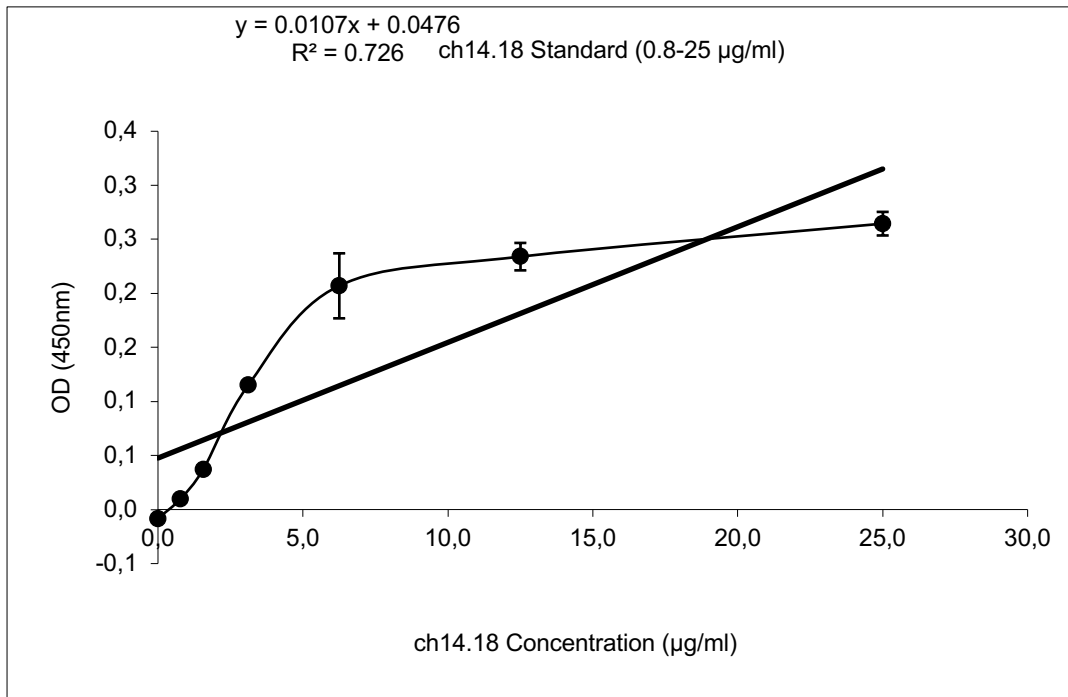


Figure 9. Standard curve representing the detectable concentration range of anti-ganglidiximab

The standard curve above represents the mean absorbance of the target protein (anti-ganglidiximab – y-axis) against a standard protein concentration. A best linear fit curve through the points in the graph is also drawn. Each point on the graph represents the mean of the four parallel titrations and its corresponding SD. A sample of known concentration (ch14.18 concentration – x-axis) is used as a positive control.

The simple linear regression model gives rise to an equation of a linear curve, in this case $y = 0.0107 * x + 0.0476$, where y is the OD at 450 nm and x is the concentration in µg/ml. The regression coefficient R^2 indicates the fit of the values into the regression model and is generally acceptable for values >0.6.

This equation is then converted to $x = (y - 0.0476) / 0.0107$ to get a concentration from the OD value obtained from the analysis of the serum of the immunized patient.

Table 11. Optical density signals in the ganglidiximab ELISA of serum taken at vaccination time points of patient SL analyzed in quadruplicates

Time Point	OD ⁴⁵⁰ values			
baseline	-0.01	-0.01	0.00	-0.01
14	0.04	0.04	0.04	0.04
28	0.11	0.11	0.11	0.09

42	0.017	0.17	0.18	0.18
56	0.43	0.44	0.44	0.44
70	0.56	0.56	0.56	0.55
84	0.61	0.63	0.62	0.63
98	0.67	0.69	0.68	0.67
112	0.66	0.65	0.65	0.64
126	0.66	0.67	0.68	0.68
140	0.68	0.67	0.68	0.68
154	0.67	0.64	0.68	0.67

¹ Optical density (OD) signals obtained from Day 0 until Day 154 and its corresponding values in quadruplicates determined using a plate reader (Synergy) HT at 450nm.

The data above were then used to calculate the concentration using the formula $x = (y - 0.0476) / 0.0107$. See Table 11.

Table 12. Concentration of the anti-ganglidximab response in the serum taken at vaccination time points of patient SL analyzed in quadruplicates

Time point ¹	Concentration (µg/ml) ²				Mean ³	SD ⁴	SEM ⁵
baseline	0.09	-0.09	0.19	-0.19	0.00	0.17	0.09
14	4.49		4.49	4.49	4.49	0.00	0.00
28	10.84	10.84	10.94		10.87	0.05	0.03
42	16.54	16.92	17.10	17.01	16.89	0.25	0.12
56	41.12	41.78	41.50	42.15	41.64	0.44	0.22
70	52.71	52.53	53.09	51.78	52.53	0.55	0.28
84	57.67	59.25	58.32	59.16	58.60	0.75	0.38
98	63.27	65.33	63.93	62.99	63.88	1.04	0.52
112	62.43	61.68	61.40	60.66	61.54	0.73	0.37
126	62.71	63.55	64.21	63.74	63.55	0.62	0.31
140	63.74	63.27	64.58	63.93	63.88	0.54	0.27
154	63.65		64.02	63.46	63.71	0.29	0.16

¹ Timepoint refers to vaccination days where serum samples were collected at 2-week intervals.

² Concentration refers to the antibody titer developed against ganglidximab at different time points (baseline to Day 154) and in various measurements.

³ Mean, also known as average or arithmetic average or the sum of the values divided by the number of values.

⁴ SD – Standard Deviation measures the amount of variation or dispersion of a set of values.

⁵ SEM – Standard Error of the Mean represents the spread of the mean of a sample of values. SEM gives a more accurate representation of the mean, while SD gives an idea of the variability of the observations.

The highlighted data are outliers and were excluded from further analysis using the outlier test according to Grubbs [122].

The mean and standard error of mean were used to plot the curve of anti-ganglidximab immune response as shown for all patients in Figure 12.

4.1.3. Anti-GD2 Immune response of SL

Finally, quantification of an anti-GD2 immune response was measured using the same standard curve used previously with known ch14.18 concentrations on the x-axis and its corresponding optical density signals on the y-axis. All samples were analyzed in triplicates, and the standard deviation was calculated from 3 values per ch14.18 concentration.

Table 13. Optical density signals of different ch14.18/CHO concentrations in the GD2 ELISA
Known ch14.18/CHO concentrations were used to create a standard curve in the GD2 ELISA (schematic see Figure 6).

Standard (OD ¹ at 450nm)		
µg/ml	MEAN ²	SD ³
25.0	0.42	0.03
12.5	0.25	0.01
6.25	0.15	0.01
3.13	0.09	0.00
1.56	0.05	0.01
0.78	0.03	0.00
0.00	0.02	0.00
blank	0.00	0.00

¹ OD – Optical Density is the colorimetric change observed in this GD2 assay, referring to the absorbance log at the chosen wavelength. The optical density is thus equivalent to the amount of captured antigen in the sample. Results are expressed as Optical Density (OD450) measurements using a microplate reader with a 450nm filter.

² Mean also known as average or arithmetic average or the sum of the values divided by the number of values.

³ SD – Standard Deviation measures the amount of variation or dispersion of a set of values.

A standard curve was produced from the above values using linear regression.

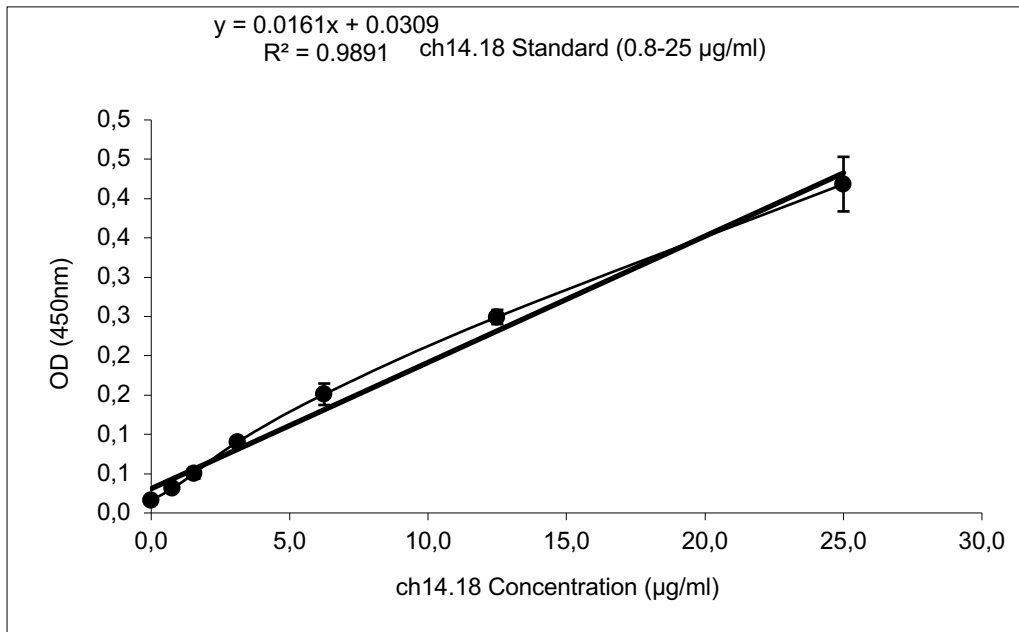


Figure 10. Standard curve representing the detectable concentration range of the anti-GD2 response

The standard curve above represents the mean absorbance of the target protein (anti-GD2 – y-axis) against a standard protein concentration. A best linear fit curve through the points in the graph is also drawn. Each point on the graph represents the mean of the three parallel titrations and its corresponding SD. A sample of known concentration (ch14.18 concentration – x-axis) is used as a positive control.

The simple linear regression model results in an equation of a linear curve, in this case $y = 0.0161 * x + 0.0309$, where y is the OD at 450 nm and x is the concentration in µg/ml. The regression coefficient R^2 indicates the fit of the values into the regression model and is generally acceptable for values >0.6 .

This equation is then converted to $x = (y - 0.0309) / 0.0161$ to acquire a concentration from the OD value obtained from the analysis of the serum of the immunized patient.

Table 14. Optical density signals in the GD2 ELISA of serum taken at vaccination time points of patient SL analyzed in quadruplicates

Time Point	OD ¹ 450 values			
baseline	0.01	0.01	0.04	0.04
14	0.01	0.01	0.00	0.00
28	0.02	0.01	0.01	0.01
42	0.01	0.01	0.01	0.01
56	0.03	0.02	0.01	0.01
70	0.04	0.03	0.01	0.01
84	0.04	0.05	0.01	0.01

98	0.04	0.03	0.01	0.01
112	0.04	0.01	0.01	0.01
126	0.01	0.01	0.01	0.01
140	0.01	0.01	0.01	0.01
154	0.01	0.01	0.01	0.01

¹ Optical density (OD) signals obtained from Day 0 until Day 154 and its corresponding values in quadruplicates determined using a plate reader (Synergy) HT at 450nm.

The data above were then used to calculate the concentration using the formula $x = (y - 0.0309) / 0.0161$. See Table 15.

Table 15. Concentration of the anti-GD2 response in the serum taken at vaccination time points of patient SL analyzed in triplicates.

Time Point ¹	Concentration ($\mu\text{g/ml}$) ²			Mean ³	SD ⁴	SEM ⁵
baseline	-0.08	-0.02	0.10	0.00	0.10	0.05
14	0.17	0.17	0.17	0.17	0.00	0.00
28		0.42	0.42	0.42	0.00	0.00
42	0.10	0.23	0.60	0.31	0.26	0.15
56	0.29	0.23	0.54	0.35	0.16	0.10
70	0.17	0.29	0.23	0.23	0.06	0.04
84	0.10	0.29	0.48	0.29	0.19	0.11
98	0.29		0.29	0.29	0.00	0.00
112	0.23	0.29	0.42	0.31	0.10	0.05
126	0.23	0.35	0.60	0.39	0.19	0.11
140	0.10	0.17	0.60	0.29	0.27	0.16
154	0.23	0.23		0.23	0.00	0.00

¹ Timepoint refers to vaccination days where serum samples were collected at 2-week intervals.

² Concentration refers to the antibody titer developed against GD2 at different time points (baseline to Day 154) and in various measurements.

³ Mean, also known as average or arithmetic average or the sum of the values divided by the number of values.

⁴ SD – Standard Deviation measures the amount of variation or dispersion of a set of values.

⁵ SEM – Standard Error of the Mean represents the spread of the mean of a sample of values. SEM gives a more accurate representation of the mean, while SD gives an idea of the variability of the observations.

The highlighted data are outliers and were excluded from further analysis using the outlier test according to Grubbs [122].

The mean and standard error of mean were used to plot the curve of anti-GD2 immune response as shown for all patients in Figure 13.

4.2. Immune response of all patients immunized with ganglidiomab

4.2.1. Anti-ganglidiomab immune response of all patients

The first parameter analyzed for all patients refers to the immune response against the protein used for vaccination, i.e., ganglidiomab. All seven patients received a test before starting the immunization to serve as their baseline levels. After the start of vaccination and in 14-day intervals (i.e., on days 14, 28, 42, 56, 70, 84, 98, 112, 126, 140, 154, and 168), each patient was sampled for monitoring of the anti-ganglidiomab immune response using the methods described previously.

Results showed that 6 of the 7 vaccinated patients showed a strong anti-ganglidiomab immune response reaching a level of $>10\mu\text{g/ml}$ already after the third vaccination (day 42) with a maximum range of 50-65 $\mu\text{g/ml}$ after six vaccinations (day 84) (Figure 11).

Only one patient did not develop a strong anti-ganglidiomab response (G-02-MN). After six vaccinations (day 84), only a background level was detected, similar to the measurement obtained at the start of vaccination. However, there was a slight signal increase after the 11th vaccination (day 168) to a concentration level of 5 $\mu\text{g/ml}$.

It is important to note that patient G-02-MN is the only patient who received a haploidentical stem cell transplantation as part of her treatment plan before entering the ganglidiomab vaccination program. This fact may explain the weak response and will be further discussed in the discussion section of this manuscript.

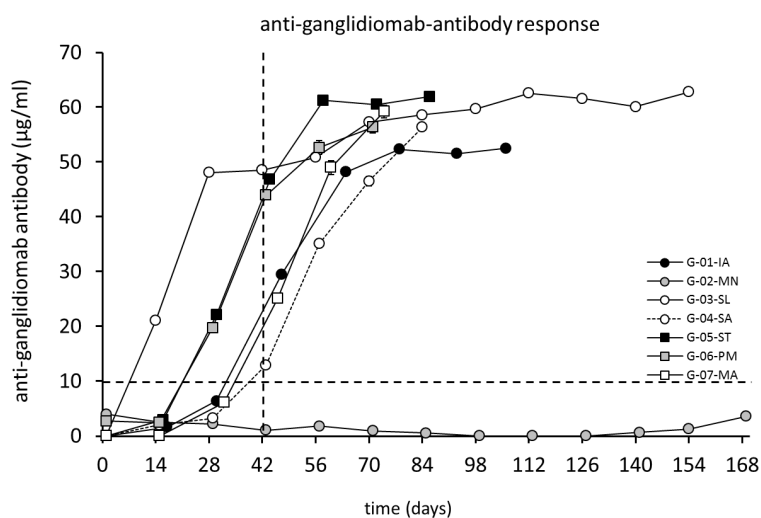


Figure 11. Induction of anti-gangliomab humoral response after vaccination with gangliomab over time

The anti-gangliomab response serum levels were analyzed through ELISA following the procedure described previously for seven patients enrolled in the vaccination program. Patients received 0.5 ml of 1mg/ml of gangliomab adsorbed to alhydrogel intramuscularly in 14-day intervals. These patients were immunized 6-22 times with gangliomab every two weeks. Patient blood samples were collected on vaccination days at the indicated time points. Graphs indicate the mean value for each patient at each time point. The standard deviation is too small to display and covered by the size of the symbol. The dashed lines indicate the 10 µg/ml value (horizontal) and the 42-day time point after three vaccinations (vertical) for illustration purposes.

4.2.2. Anti-ganglidiximab immune response of all patients

The second parameter analyzed is the immune response generated against the chimeric Ab ganglidiximab, which consists of the same murine variable regions as gangliomab genetically fused to human constant regions of IgG1. Similar to the procedure done with gangliomab, all patients received a blood test to check baseline values before receiving the gangliomab vaccine. In addition, blood samples were also collected every 14 days to monitor the anti-ganglidiximab immune response following the previously described methods.

Analogous to the response against gangliomab, the results in this second analysis showed that 6 of the 7 vaccinated patients developed an anti-ganglidiximab immune response. Patient G-02-MN, who had a haploidentical blood stem cell transplantation, continued to show no response. Compared to the first analysis, patients tested with this assay generally displayed a slower immune response. For example, at the 42-day time point (after the third vaccination,

Figure 12), only three patients reached an anti-ganglidiximab level of >10µg/ml. In contrast to the anti-ganglidiomab response wherein six patients have already achieved this level at the same time point (Figure 11).

Also, the maximum Ab levels (30-65 µg/ml) reached after receiving 5-7 vaccinations (days 70-98) were lower compared to the response level seen against ganglidiomab.

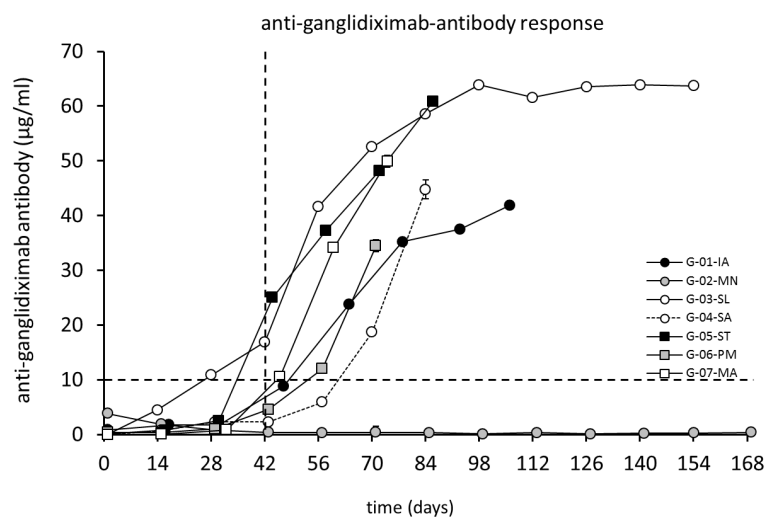


Figure 12. Induction of anti-ganglidiximab humoral response after vaccination with ganglidiomab over time

The anti-ganglidiximab response serum levels were analyzed through ELISA following the procedure described previously. Graphs indicate the mean value for each patient at each time point. The standard deviation is too small to display and covered by the size of the symbol. The dashed lines indicate the 10 µg/ml level (horizontal) and the 42-day time point after three vaccinations (vertical) for illustration purposes.

4.2.3. Anti-GD2 immune response of all patients

The immune response generated against the GD2 antigen is displayed in the graph below. In contrast to the previous two analyses, immune response against GD2 was shown to be significantly weaker, with maximum antibody levels only reaching 2.5 µg/ml. Two patients G-04-SA and G-01-IA, showed max Ab responses on day 14 and day 84, respectively. The response of patient G-04-SA, in particular, was only short-lived with a relatively wide standard deviation, and levels falling below 1 µg/ml on day 28 and reaching zero or no response on day 56. Patient G-03-SL, on the other hand, displayed an immune response starting on day 14 until

the end of the vaccination period; however, all measured Ab levels were below 1 µg/ml. Finally, patient G-02-MN showed no response with a weak signal (<1 µg/ml) on day 0 before the first vaccination, eventually falling to null values for the rest of the vaccination period, consistent with the non-response observed in the patient’s ganglidiomab and ganglidiximab ELISA methods.

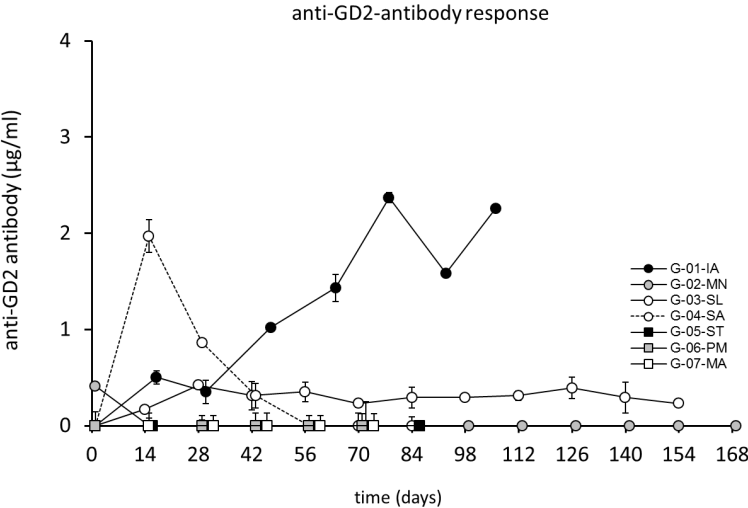


Figure 13. Induction of anti-GD2 humoral response after vaccination with ganglidiomab over time

The anti- GD2 response serum levels were analyzed through ELISA following the procedure described previously for the seven patients immunized with the ganglidiomab vaccine. Graphs indicate the mean value for each patient at each time point. The standard deviation can be seen in some of the values presented in the graph.

4.2.4. Complement dependent cytotoxicity of all patients

Similar to the anti-GD2 response, a mixed pattern was observed for the GD2 specific CDC activity of immunized patients (Figure 14). Patients G-01-IA and G-04-SA developed a CDC response consistent with findings in the GD2, ganglidiomab, and ganglidiximab ELISA methods, suggesting that the vaccine performed as anticipated. However, there were also unexpected results in the CDC response. For instance, patient G-03-SL, who had detectable levels of anti-GD2 antibodies in the serum (Figure 13), did not develop a CDC response (Figure 14). And vice versa, patient G-02-MN, who showed no response in any ELISA method, had a measurable CDC response already on day 0, which on day 14 showed a steep drop to levels

below 40% and another rise in levels (>40%) on day 90, eventually falling to levels below 20% after day 90. Although the CDC levels of G-02-MN depicted on days 20, 50, and 90 showed a relatively wide margin of error. The absence of a CDC response in patients G-05 ST, G-06 PM, and G-07 MA is again consistent with the lack of a signal in their GD2 ELISA.

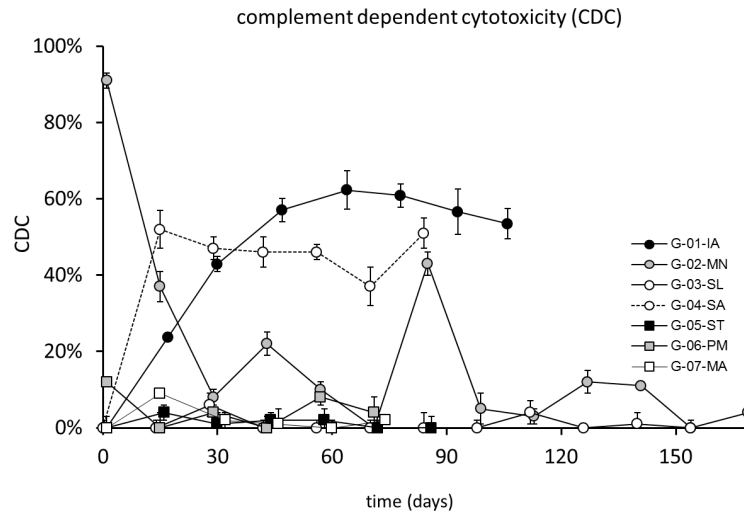


Figure 14. CDC activity in the sera of immunized patients

Blood samples are collected on the indicated days, as shown in the above figure. Sera of the seven patients were then analyzed using calcein-AM-based cytotoxicity assay as described in the previous section. Percent activity is depicted in the above figure for each patient.

Y axis – CDC % of target cell lysis

X axis – vaccination time points

4.2.5. Mean CDC activity of all patients

Below is the average CDC activity of all patients during the entire vaccination period (Figure 15). Notable is the steady increase in the percent activity over time, but with a wide standard deviation for the values depicted after day 40.

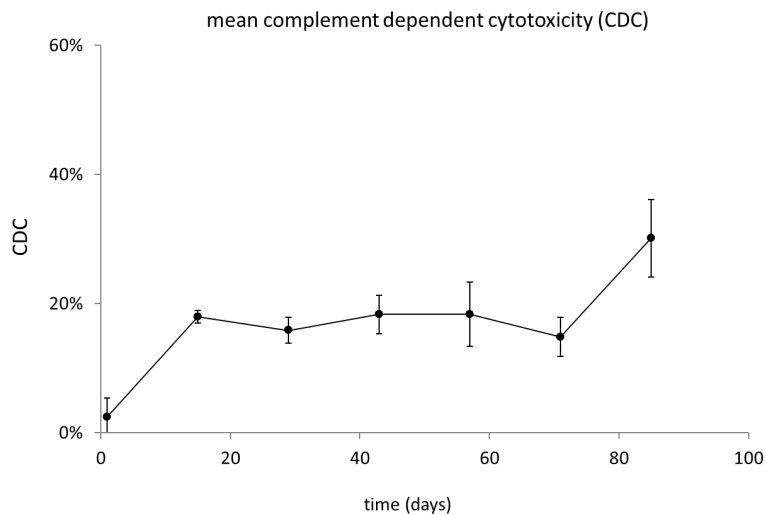


Figure 15. Mean CDC activity in the sera of all immunized patients

Blood samples are collected on the indicated days, as shown above. Sera of the seven patients were then analyzed using calcein-AM-based cytotoxicity assay, and the mean CDC percent of lysis was calculated.

4.2.6. Survival of immunized patients

The date of diagnosis, date of the first vaccine, date of the last follow-up, and patient status are shown in the following table (Table 16). The range between the first dose of vaccine given until the last follow-up date was determined among the patients enrolled in this program, resulting in a median value of 56 months and 16 days for the entire cohort.

From this group of patients, two had a relapse or progression of their disease (MN and SA, see Table 6), while the rest were frontline patients. The frontline patients had an overall median range of 56 months and 16 days from their first vaccine dose to their last follow-up date, which is also the range for the entire group. In comparison, the range for the two relapsed patients is 56 months and 20 days for SA and 16 months and 19 days for MN from their first vaccine dose to their last follow-up date or date of death.

No significant side effects were observed. This observational data suggest that vaccination with ganglidiomab may result in long-term and disease-free survival.

Table 16. Patient status and range of the first vaccine dose to the last follow-up

Patient	Date of Diagnosis	Date of first vaccination	Date of last vaccination	Date of last follow-up	Range from first dose to last follow-up	Patient status
IA	10/2010	20/11/2012	07/03/2013	26/07/2019	80 months, 7days	alive without disease
MN ¹	01/2010	22/05/2013	12/03/2014	10/10/2014 ²	16 months, 19 days	dead
SL	05/2011	25/03/2014	26/08/2014	28/06/2019	63 months, 4 days	alive without disease
SA ¹	02/2012	12/11/2014	07/01/2015	31/07/2019	56 months, 20 days	alive without disease
ST	01/2013	03/11/2014	21/01/2015	18/11/2018	48 months, 16 days	alive without disease
PM	05/2013	17/11/2014	26/01/2015	01/08/2019	56 months, 16 days	alive without disease
MA	06/2012	14/11/2014	09/02/2015	01/07/2015	7 months, 18 days	alive without disease

¹ Patients with relapsed high-risk neuroblastoma

² Date of last follow-up refers to the patient's date of death, which was unrelated to neuroblastoma

5. Discussion

Anti-GD2 antibodies have been known to improve the outcome of children with high-risk neuroblastoma [59]. However, passive immunotherapy loses efficacy once the treatment cycles are completed. Developing a vaccine that can provide a sustained anti-tumor response for immunized patients with prolonged protection from relapse may be the answer to this gap in therapy. The ganglidiomab vaccine was thus developed and tested in seven patients with high-risk neuroblastoma and evaluated for its ability to stimulate an immune response.

The evolution of treatment options for HR-NB has led to the addition of immunotherapy to the current standard of care. The advent of monoclonal antibodies has indeed revolutionized the care of neuroblastoma patients. However, there is still a need for innovative treatment methods for patients with refractory or relapsed high-risk diseases.

5.1. Passive Immunotherapy

Passive mAb therapy (dinutuximab, dintuximab-beta) has seen success in its use against HR-NB due in part to the sensitivity of neuroblastoma to CDC and ADCC, which is unusual among most solid tumors. The likely reason for this is the downregulation or absence of HLA (Human Leucocyte Antigen), leading to a lack of ligands for the immunoglobulin-like receptors facilitating the activity of natural killer cells during ADCC [123]. In 2020, the arsenal of GD2-specific antibody therapies grew by the addition of naxitamab combined with GM-CSF, which the FDA approved for relapsed or refractory HR-NB patients in the bone or bone marrow who have demonstrated a partial response, minor response, or stable disease to previous therapy [124]. Naxitamab is a humanized anti-GD2 IgG1k monoclonal antibody that has been shown to achieve a complete response rate of 67% and an overall response rate of 75% in a high-risk patient population [125]. This humanized version retains the binding specificity to ganglioside GD2 similar to dinutuximab and dinutuximab-beta but is 98% human. Naxitamab was designed to reduce the occurrence of HACAs while preserving CDC potency through its high affinity for GD2 and intensifying ADCC through the human IgG1-Fc [126].

However, the outcome of children with HR-NB is still characterized by a high frequency of relapse in 40-50% of cases despite passive immunotherapy [127]. The still relatively high relapse rate may be related to the temporary effect of infused immunoglobulins, which lose their activity after clearance from the blood stream. Therefore further improvements to the treatment concept of passive immunotherapy are necessary.

5.2. Combination immunotherapies with anti-GD2-antibodies

One option to improve the efficacy of passive immunotherapy lies in innovative combinations of anti-GD2 antibodies with other immunotherapeutic interventions with the goal to increase the anti-neuroblastoma activity and the duration of the response. For instance, recent studies show that the use of PD-1/PD-L1 checkpoint inhibitors may intensify the effect of passive immunotherapy with ch14.18/CHO (dinutuximab-beta) [128].

Programmed Death 1 (PD-1) is an important immune checkpoint receptor expressed by activated T cells and NK cells. PD-1 binds to its ligands PD-L1, expressed by activated hematopoietic cells and epithelial cells, and PD-L2, displayed by macrophages and dendritic cells, leading to immunosuppressive activity. PD-L1 expression was examined through immunohistochemistry and was seen to be positive in 72% of patients with high-risk NB [128]. Thus, NB cells express ligand of the immune checkpoint receptor PD-1 and thus inhibit the anti-tumor immune response. In one study, anti-tumor effects from ch14.18/CHO were found to increase by blocking the immune checkpoint pathway PD-1/PD-L1 [128, 129].

This combination is particularly noteworthy because the PD-1/PD-L1 checkpoint is upregulated in preclinical neuroblastoma models upon treatment with dinutuximab-beta [129]. This effect can be considered an escape mechanism by the tumor to protect malignant cells from immune attacks. Therefore the combined treatment of dinutuximab-beta with PD-1/PD-L1 checkpoint inhibitor has a synergistic anti-tumor effect that may also increase efficacy in the clinical setting.

5.3. Adoptive transfer of GD2 specific chimeric antigen receptor (CAR) T cells

One evolving therapeutic strategy against NB is the adoptive transfer of chimeric antigen receptor (CAR) T cells, which has been successful in treating acute lymphoblastic leukemia. These cells combine the specificity of an antibody with the apoptotic capacity of T cells in a manner that is independent of MHC [130]. CAR-T cell therapy for NB has proven to be safe and feasible, but significant barriers to efficacy remain. These include the absence of T cell longevity, challenges in target identification, and an immunosuppressive tumor milieu [130].

In a phase 1 study treating 12 children with relapsed NB with second-generation GD2-specific CAR-T cells, the results showed no objective clinical response after 28 days of CAR-T cell infusion. Nevertheless, two of the six patients receiving a higher dose after conditioning chemotherapy experienced grade 2 to 3 cytokine release syndrome, and three exhibited soft tissue and bone marrow disease regression [131].

With new advances in CAR-T cell engineering, many of the issues mentioned above are currently being addressed. Once some key problems are solved, this strategy could contribute to further improving outcomes.

5.4. Adaptive immunotherapy using vaccines

5.4.1 Vaccines based on gangliosides

Finally, active immunotherapy or cancer vaccines have been named the “next generation” strategy to overcome the short-lived immune response seen after administering monoclonal antibodies and CAR-T cells. A bivalent vaccine, which is protein-free and lipid-free, is currently being evaluated in clinical trials that target two proteins found on neuroblastoma cells: GD2L and GD3L [89]. In this trial, a total of 102 patients with HR-NB who achieved remission after receiving salvage therapies were enrolled. Subjects then received seven subcutaneous injections of GD2/GD3 vaccine combined with oral β -glucan as immunostimulator after the third dose of the vaccine. Combining subcutaneous GD2/GD3 conjugate vaccine with oral β -glucan adjuvant was found to be safe and effective in producing antibody response which is associated with the biomarker, dectin-1 receptor single nucleotide polymorphism rs901533. The progression-free survival (PFS) was $32\% \pm 6\%$, and the overall survival was $71\% \pm 7\%$ at five years [132]. Furthermore, an induction of persistent anti-GD2 and anti-GD3 antibody responses was observed, and a high anti-GD2 IgG1 titer was found to be independently correlated with favorable results.

Although these data look interesting and promising, the use of carbohydrates as an antigen has major disadvantages; since the immune response is not induced following classical antigen presentation pathways, it is T-cell independent and, thus, short-lived.

Therefore, developing a vaccine that can provide a sustained anti-tumor response for immunized patients with prolonged protection from relapse may be advantageous. The concept of mimotope vaccines overcomes this hurdle of T-cell independence by using peptides or proteins that mimic the carbohydrate structure of GD2.

5.4.2 GD2 mimotope vaccines

The ganglidiomab vaccine is a mimic of GD2 and was developed and tested in seven patients with high-risk neuroblastoma and evaluated for its ability to stimulate an immune response.

The response against the vaccine (i.e., ganglidiomab) was excellent when tested by ganglidiomab ELISA (Figure 11), except for one patient (G02-MN) who had a haploidentical stem cell transplantation as part of the previous treatment.

A haploidentical stem cell transplantation procedure is based on the use of a parent as a donor source for the hematopoietic blood stem cells. These stem cells are harvested from the blood of one parent by leukapheresis containing large amounts of T-cells and B-cells. These immune cells are unsafe for the recipient as they may elicit a severe graft-versus-host response in the haploidentical transplant setting. Therefore, T-cells and B-cells are removed from the graft by depleting CD3- (T-cell marker) and CD19- (B-cell marker) positive cells using the CliniMACS technology [133].

Although patients who receive a CD3/CD19 depleted stem cell graft have a very low incidence of graft versus host disease (GvHD) [118], they also have a prolonged recovery of their immune system with a long-lasting B-cell deficiency following the transplant [134]. Since the vaccination with ganglidiomab and the subsequent induction of a B-cell response requires both a functional B- and T-cell compartment, the haploidentical transplantation provides a mechanistic explanation why this patient showed nearly no response following ganglidiomab vaccination.

As to the ganglidiximab antibody response, patients still showed a good albeit slower response with a lower final Ab level than the response generated by ganglidiomab (Figures 11 and 12). This is primarily due to ganglidiximab's chimeric property, characterized by a fully human Fc portion and a murine variable region. Therefore, serum antibodies from immunized patients binding to the vaccine's murine Fc region were not detected when using ganglidiximab as a capture antibody.

Finally, the discrepancy between anti-ganglidiomab and anti-ganglidiximab response compared to the anti-GD2 response exhibited by 4 out of the 7 patients can be either due to methodological or conceptual reasons (Figures 11-13).

5.5. Methodological challenges for the detection of a GD2 specific immune response

On the methodological side, ELISA assays have long been established as a powerful tool to quantify antibody titers in complex mixtures. Although this plate-based assay technique has a robust nature, exhibits exceptional sensitivity, is quick and easy to perform, it is not free from errors. Problems may arise when insufficient washing or incorrect dilutions are prepared. This can then result in negative or suboptimal results. High inter-well variability can also occur by mistakes in sample preparation and pipette inconsistencies. Data with high variation (or, in our case, outliers) can skew the results and give rise to discrepancies in the overall outcome. Measures to prevent such occurrences or means that standardize procedures are therefore necessary to ensure quality in the data collection.

Furthermore, ELISA methods with a coating of GD2 to the well are complicated because glycolipids do not have the same coating properties as proteins. Therefore wash steps may disturb the adhesion of the GD2 to the plastic surface of the 96 well plates used. One possibility of solving this methodological obstacle is using a different technique to analyze the GD2 response, such as Biacore. Biacore allows the detection of interactions between GD2 and proteins based on the surface plasmon resonance, an optical phenomenon that enables identifying real-time interactions [135]. There are also specific biosensors optimized for glycolipids to be used on the solid phase of the sensor, which can characterize molecular interactions in terms of both affinity and kinetics [136]. It will be subject to future work to investigate the response observed in patients with this technique.

5.6. Role of vaccine design to elicit optimal GD2 response

5.6.1 Selection of adjuvant

A conceptual reason for the suboptimal response showed by some of the patients could lie in the nature of the developed vaccine. On the one hand, this may be caused by the choice of adjuvant used in its development. Aluminum-based vaccine adjuvants have been well established since the 1920s, mainly because of their notable immunostimulatory properties and their capacity to attach to proteins for an effective presentation to the immune system during vaccination [137]. Consequently, it has become the gold standard against which all new adjuvants need to be compared. Alhydrogel, an aqueous aluminum hydroxide (alum) suspension, has been extensively used as a protein-binding vaccine adjuvant for many years [138].

Despite its proven immunogenicity, the adjuvant's interaction with the protein vaccine in question needs to be examined thoroughly as well as in the final product. This individual examination of each vaccine component and the overall outcome is vital in vaccine production and has been a pharmaceutical requirement in the past years. A growing alternative, especially among aluminum-based vaccines that have failed, is the use of water-in-oil formulation adjuvants. This emulsion type of enhancer, specifically the Incomplete Freund's Adjuvant (IFA), has been widely used in human research and has been shown to increase antibody responses while also being well-tolerated [139]. Toxicity associated with its use has been curbed through the use of high-grade oils and surfactants, with further testing still ongoing today. It can also be mixed in conjunction with other active compounds such as saponins and cytokines [139].

In recent years IFA has been reformulated and has been used in experimental cancer vaccines. In one study using IFA (Montanide ISA-51 VG) as an adjuvant for a multi-peptide melanoma vaccine, CD8⁺ and CD4⁺ T cell responses were shown to be preserved, thereby proving the chosen adjuvant's immunogenicity [140]. In a more recent study, IFA was found to create an immense antigen depot combined with toll-like receptor agonists to activate antigen-presenting cells (APC) and a tetanus peptide that can induce CD4⁺ helper T cell responses. In this trial, T cell responses to the tetanus helper peptide were more significant when combined with IFA than without it [141]. Therefore, the effect of IFA is not only seen in the activation of CD8⁺ T cells but also in the activation of CD4⁺ T cells and the subsequent APC activation.

Another adjuvant available for human use is β -glucan. Research done with glucan-based vaccines has shown its ability to stimulate the production of granulocytes, monocytes, macrophages, and natural killer cells[142]. β -glucans have been known to modify biological responses when used as an immunoadjuvant therapy for cancer since the 1980s. Its immunogenic features are brought primarily about by its molecular structure. They are first recognized as pathogen-associated molecular patterns by immune cell receptors on macrophages, neutrophils, and dendritic cells such as toll-like receptors, dectin-1, CR3, and CD5. These interactions then prompt the activation of intracellular signaling followed by the expression of immune molecular factors controlling non-specific and specific immune responses [143].

Therefore, the selection of adjuvant to be used and its effects critical to the induction of anti-tumor T cell responses to a vaccine remains crucial in the development of a set of updated adjuvants for diverse types of vaccines.

5.6.2 Structure of the antigen used for the vaccine (Peptide-mimotopes)

The structure of the antigen used for the vaccine design may also explain the results observed. The part of the anti-idiotypic antibody ganglidiomab that serves as a mimic for the nominal antigen GD2 is a relatively small part of the immunoglobulin molecule, i.e., the complementarity-determining region (CDR). The other parts of the ganglidiomab immunoglobulin molecule are not needed for the desired GD2 specific response. Hence other ways of mimotope vaccine designs need to be explored, for example, by using only short peptides that mediate the mimotope function.

Mimotopes are epitope-mimicking peptide structures that can be identified by phage display technology and further optimized by SPOT synthesis [144], a sequential application of systematic amino acid substitution. When mimetic peptides are used for immunizations, they induce desired antibody responses solely based on the principle of molecular mimicry [103, 106, 145]. They can also overcome the T cell independence of carbohydrate antigens, which provides an alternative option to glycoconjugates or anti-idiotypic antibodies as vaccines.

In this context, a GD2 mimetic peptide identified by phage display technology was subjected to further optimization. The original mimotope was identified from a phage display peptide library that expresses circular decapeptides fused to the virion coat protein pIII of the filamentous phage M13 [146]. It was later shown that DNA immunization with this circular GD2 mimotope peptide was effective in reducing spontaneous liver metastases in a syngeneic mouse model [103]. To further optimize the vaccination effect, the peptide-mimotope was systematically altered by exchanging amino acids at defined positions of the original mimotope to create mutants using SPOT synthesis. The resulting peptides were tested for GD2 mimicry, and a new peptide was identified with an improved mimotope characteristic (i.e., C3 peptide mimotope). Utilizing this C3 mimotope as a vaccine resulted in an 18-fold increase in the anti-GD2 serum response associated reducing primary tumor growth and spontaneous metastasis in contrast to the original mimotope controls in a syngeneic neuroblastoma [106].

A similar phage library approach was used to characterize linear peptides of 15 amino acids in length (phage display peptide library X15) which led to the isolation of mimetic peptide 47. This peptide was able to elicit GD2 cross-reactive IgG antibody responses, and DNA vaccine-induced antibodies recognized GD2-positive tumor cells, mediated complement-dependent cytotoxicity, and exhibited protection against GD2-positive melanoma growth in a severe immunodeficient mouse xenograft model [147]. This peptide was also further optimized to improve the mimotope function. In this case, an *in silico* modeling approach was selected using the template structures of VH and VL domains of anti-GD2 antibody ch14.18. The binding affinity of mutated peptide variants of peptide 47 was calculated using molecular modeling programs. This sequential procedure led to the 47-LDA mutant with an increased mimicry to GD2, as shown in preclinical models [147].

In both examples using the circular and the linear peptide mimotope, a sequential approach of peptide identification followed by optimization was proven to be successful. This method may therefore provide a strategy to optimize the efficacy of the GD2 peptide mimotope of ganglidiomab.

The strategy of mimotope vaccination was also tested for other antigens, such as the immune checkpoint programmed cell death 1 (PD1). Peptides covering the extracellular domains of human PD1 (hPD1) were used to identify hPD1-derived mimotopes [148]. The identified mimotopes derived from PD1 were then shown to significantly hinder the mAbs' (Nivolumab) capacity in preventing PD1/PD-L1 interactions. A reduction in tumor growth *in vivo* was consequently seen following active immunization with the mouse PD1-derived (mPD1-derived) mimotope, with an associated significant decrease in proliferation as well as increased apoptotic rates in the tumors. Moreover, the combination of vaccinating with the mPD1-derived mimotope and a multiple B-cell epitope vaccine enhanced the vaccine's anti-tumor effect [148]. These results suggest that active immunization with mimotopes of immune checkpoint inhibitors can be used as a stand-alone therapy or in combination with tumor-specific vaccines and underlines the usefulness of the peptide mimotope approach in immunotherapy of cancer.

5.7. Outcome of patients vaccinated with ganglidiomab

Since the introduction of dinutuximab-beta for treating patients with HR-NB, an improvement in the event-free and overall survival has been seen, solidifying the benefits of immunotherapy for the treatment of a solid tumor in childhood [78].

In the phase 3 multicenter, randomized trial studying the effect of dinutuximab-beta with IL-2 and dinutuximab-beta alone among eligible patients with the primary endpoint being a 3-year event-free survival, EFS was found to be 56% (95% CI 49–63) among patients assigned to dinutuximab-beta, compared with 60% (95% CI 53–66) for patients in the dinutuximab-beta plus subcutaneous IL-2 group [78]. Since all of the patients enrolled in our compassionate program received antibody therapy with IL-2 with or without RA, adding ganglidiomab in the armamentarium against NB can potentially increase the EFS and OS of immunized patients. In our compassionate use program, we did not observe any disease-related death following vaccination with ganglidiomab with a median observation time of 56 months and 16 days for the entire cohort and for the five frontline patients.

Since this cohort included five frontline patients and two patients (MN and SA) with relapse/refractory neuroblastoma, we evaluated them separately.

As mentioned above, the five frontline patients did not show any progression of their disease after receiving the ganglidiomab vaccine. The median range from their first dose to the last follow-up date is 56 months and 16 days. Although this does not permit a direct comparison with the findings in the above clinical trial, the observation suggests a benefit of the vaccine for long-term survival and warrants further investigations.

Comparing our results to historical controls of relapsed HR-NB, a survival benefit is also suggested following vaccination with ganglidiomab. Among the patients enrolled in our compassionate use program, two (MN and SA) were also diagnosed with relapsed/refractory NB and accordingly received further treatment for their relapse/progression before receiving ganglidiomab. For MN, the time to the last follow-up (here refers to the date of death unrelated to neuroblastoma) from the initial diagnosis was 57 months, whereas the time from the first vaccine dose to the last follow-up was 16 months and 19 days. On the other hand, SA had a time to follow-up from the date of diagnosis of about 89 months, and the time from the first vaccine dose to the last follow-up was determined at 56 months and 20 days. In contrast to the data derived from a cohort of patients with recurrent/refractory neuroblastoma from Children's Oncology Group (COG) modern-era early-phase trials study wherein the time to progression (TTP) was found to be only 58 days [149]. This comparison suggests that even among relapsed/refractory NB patients, vaccination with ganglidiomab may provide a survival benefit.

6. Summary

Patients diagnosed with HR neuroblastoma have an extremely poor long-term prognosis. Therefore, new therapeutic agents to address this problem are needed. We report the development of an anti-idiotypic vaccine (ganglidiomab) against the tumor-associated antigen disialoganglioside GD2 and studied the immune response among seven vaccinated patients enrolled in our compassionate use program.

All seven patients were injected with the ganglidiomab vaccine (6-22 injections) every two weeks. Each subcutaneous injection contained 0.5mg of ganglidiomab and 1.67mg aluminum as adjuvant. We then determined the patient's immune response against ganglidiomab, ganglidiximab, and GD2 using ELISA methods. All patients showed a good response against ganglidiomab and ganglidiximab. However, GD2 immune response was only detectable in 2 patients (with maximum Ab levels of 2.5µg/ml).

These discrepancies in the patients' immune responses could be due to methodological (ELISA) reasons, vaccine properties, including the type of adjuvant used, and the antigen structure used for the vaccine itself. Of recent interest is the use of mimetic peptides for immunizations to produce the wanted antibody responses. Using the phage display technique, a mimetic peptide vaccine was developed and further improved. Pilot studies testing this vaccine showed significant anti-GD2 serum response associated with a reduction in tumor growth and spontaneous metastasis. This particular method could thus help in the optimization of the efficacy of the GD2 peptide mimotope of ganglidiomab.

In terms of outcome, all immunized patients did not experience a relapse of their neuroblastoma with a median range of 56 months and 16 days from their first dose of the vaccine to their last follow-up, which contrasts to what is known from historical control cohorts.

This is the first in man use of the anti-idiotypic vaccine ganglidiomab to improve the survival among HR-NB patients with or without a history of relapse and provides important baseline data to evaluate the vaccine in prospective clinical trials.

7. References

1. Zage, P.E., *Novel Therapies for Relapsed and Refractory Neuroblastoma*. Children (Basel), 2018. **5**(11).
2. Cheung, N.K. and M.A. Dyer, *Neuroblastoma: developmental biology, cancer genomics and immunotherapy*. Nat Rev Cancer, 2013. **13**(6): p. 397-411.
3. Lode, H.N., et al., *Vaccination with anti-idiotypic antibody ganglidiomab mediates a GD(2)-specific anti-neuroblastoma immune response*. Cancer Immunol Immunother, 2013. **62**(6): p. 999-1010.
4. Armideo, E., C. Callahan, and L. Madonia, *Immunotherapy for High-Risk Neuroblastoma: Management of Side Effects and Complications*. J Adv Pract Oncol, 2017. **8**(1): p. 44-55.
5. Yu, A.L., et al., *Anti-GD2 antibody with GM-CSF, interleukin-2, and isotretinoin for neuroblastoma*. N Engl J Med, 2010. **363**(14): p. 1324-34.
6. Camisaschi, C., et al., *Immune landscape and in vivo immunogenicity of NY-ESO-1 tumor antigen in advanced neuroblastoma patients*. BMC Cancer, 2018. **18**(1): p. 983.
7. Mosse, Y.P., et al., *Identification of ALK as a major familial neuroblastoma predisposition gene*. Nature, 2008. **455**(7215): p. 930-5.
8. Trochet, D., et al., *Molecular consequences of PHOX2B missense, frameshift and alanine expansion mutations leading to autonomic dysfunction*. Hum Mol Genet, 2005. **14**(23): p. 3697-708.
9. Souttou, B., et al., *Activation of anaplastic lymphoma kinase receptor tyrosine kinase induces neuronal differentiation through the mitogen-activated protein kinase pathway*. J Biol Chem, 2001. **276**(12): p. 9526-31.
10. Pugh, T.J., et al., *The genetic landscape of high-risk neuroblastoma*. Nat Genet, 2013. **45**(3): p. 279-84.
11. Chen, Y., et al., *Oncogenic mutations of ALK kinase in neuroblastoma*. Nature, 2008. **455**(7215): p. 971-4.
12. Lin, J.J., G.J. Riely, and A.T. Shaw, *Targeting ALK: Precision Medicine Takes on Drug Resistance*. Cancer Discov, 2017. **7**(2): p. 137-155.
13. Stermann, A., et al., *Targeting of MYCN by means of DNA vaccination is effective against neuroblastoma in mice*. Cancer Immunol Immunother, 2015. **64**(10): p. 1215-27.
14. Huang, M. and W.A. Weiss, *Neuroblastoma and MYCN*. Cold Spring Harb Perspect Med, 2013. **3**(10): p. a014415.
15. Maris, J.M., et al., *Evidence for a hereditary neuroblastoma predisposition locus at chromosome 16p12-13*. Cancer Res, 2002. **62**(22): p. 6651-8.
16. Carlson, L.-M., *Interactions between Neuroblastoma and the Immune System - Cellular pathways and Mediators*. 2011, Karolinska Institutet Stockholm.
17. Chu, C.M., et al., *Clinical presentations and imaging findings of neuroblastoma beyond abdominal mass and a review of imaging algorithm*. Br J Radiol, 2011. **84**(997): p. 81-91.
18. Smith, S.J., et al., *Incidence of pediatric Horner syndrome and the risk of neuroblastoma: a population-based study*. Arch Ophthalmol, 2010. **128**(3): p. 324-9.
19. O'Brien, R.T., et al., *Superior vena cava syndrome in children*. West J Med, 1981. **135**(2): p. 143-7.

20. DuBois, S.G., et al., *Metastatic sites in stage IV and IVS neuroblastoma correlate with age, tumor biology, and survival*. J Pediatr Hematol Oncol, 1999. **21**(3): p. 181-9.
21. Swift, C.C., et al., *Updates in Diagnosis, Management, and Treatment of Neuroblastoma*. Radiographics, 2018. **38**(2): p. 566-580.
22. Hero, B., et al., *Metastatic neuroblastoma in infancy: what does the pattern of metastases contribute to prognosis?* Med Pediatr Oncol, 2000. **35**(6): p. 683-7.
23. Shown, T.E. and M.F. Durfee, *Blueberry muffin baby: neonatal neuroblastoma with subcutaneous metastases*. J Urol, 1970. **104**(1): p. 193-5.
24. Zhang, Y., et al., *Clinical characteristics of infant neuroblastoma and a summary of treatment outcome*. Oncol Lett, 2016. **12**(6): p. 5356-5362.
25. Maris, J.M., et al., *Neuroblastoma*. Lancet, 2007. **369**(9579): p. 2106-20.
26. Matthay, K.K., et al., *Treatment of high-risk neuroblastoma with intensive chemotherapy, radiotherapy, autologous bone marrow transplantation, and 13-cis-retinoic acid*. Children's Cancer Group. N Engl J Med, 1999. **341**(16): p. 1165-73.
27. Gesundheit, B., et al., *Ataxia and secretory diarrhea: two unusual paraneoplastic syndromes occurring concurrently in the same patient with ganglioneuroblastoma*. J Pediatr Hematol Oncol, 2004. **26**(9): p. 549-52.
28. Zhang, Y.T., et al., *Different Kinds of Paraneoplastic Syndromes in Childhood Neuroblastoma*. Iran J Pediatr, 2015. **25**(1): p. e266.
29. Sokol, E. and A.V. Desai, *The Evolution of Risk Classification for Neuroblastoma*. Children (Basel), 2019. **6**(2).
30. Pinto, N.R., et al., *Advances in Risk Classification and Treatment Strategies for Neuroblastoma*. J Clin Oncol, 2015. **33**(27): p. 3008-17.
31. Evans, A.E., G.J. D'Angio, and J. Randolph, *A proposed staging for children with neuroblastoma*. Children's cancer study group A. Cancer, 1971. **27**(2): p. 374-8.
32. Brodeur, G.M., et al., *International criteria for diagnosis, staging, and response to treatment in patients with neuroblastoma*. J Clin Oncol, 1988. **6**(12): p. 1874-81.
33. Ikeda, H., et al., *Experience with International Neuroblastoma Staging System and Pathology Classification*. Br J Cancer, 2002. **86**(7): p. 1110-6.
34. Monclair, T., et al., *The International Neuroblastoma Risk Group (INRG) staging system: an INRG Task Force report*. J Clin Oncol, 2009. **27**(2): p. 298-303.
35. Cohn, S.L., et al., *The International Neuroblastoma Risk Group (INRG) classification system: an INRG Task Force report*. J Clin Oncol, 2009. **27**(2): p. 289-97.
36. Matthay, K.K., et al., *Criteria for evaluation of disease extent by (123)I-metaiodobenzylguanidine scans in neuroblastoma: a report for the International Neuroblastoma Risk Group (INRG) Task Force*. Br J Cancer, 2010. **102**(9): p. 1319-26.
37. Ambros, P.F., et al., *International consensus for neuroblastoma molecular diagnostics: report from the International Neuroblastoma Risk Group (INRG) Biology Committee*. Br J Cancer, 2009. **100**(9): p. 1471-82.
38. Beiske, K., et al., *Consensus criteria for sensitive detection of minimal neuroblastoma cells in bone marrow, blood and stem cell preparations by immunocytology and QRT-PCR: recommendations by the International Neuroblastoma Risk Group Task Force*. Br J Cancer, 2009. **100**(10): p. 1627-37.
39. Seeger, R.C., *Immunology and immunotherapy of neuroblastoma*. Semin Cancer Biol, 2011. **21**(4): p. 229-37.
40. Hellstrom, I.E., et al., *Demonstration of cell-bound and humoral immunity against neuroblastoma cells*. Proc Natl Acad Sci U S A, 1968. **60**(4): p. 1231-8.

41. Evans, A.E., J. Gerson, and L. Schnauffer, *Spontaneous regression of neuroblastoma*. Natl Cancer Inst Monogr, 1976. **44**: p. 49-54.
42. Bill, A.H., *Immune aspects of neuroblastoma*. Current information. Am J Surg, 1971. **122**(2): p. 142-7.
43. Klenk, E. and W. Gielen, *Untersuchungen Über Die Konstitution Der Ganglioside Aus Menschengehirn Und Die Trennung Des Gemischs in Die Komponenten*. Hoppe-Seylers Zeitschrift Fur Physiologische Chemie, 1961. **326**: p. 144-&.
44. Svennerholm, L., *Ganglioside designation*. Adv Exp Med Biol, 1980. **125**: p. 11.
45. Kudva, A.a.M., Shakeel *Chapter 9 - Immunotherapy for Neuroblastoma*, in *Neuroblastoma*, S. Ray, Editor. 2019, Academic Press: Cambridge, Massachusetts, United States. p. 147-173.
46. Sait, S. and S. Modak, *Anti-GD2 immunotherapy for neuroblastoma*. Expert Rev Anticancer Ther, 2017. **17**(10): p. 889-904.
47. Lammie, G.A., et al., *Ganglioside Gd(2) Expression in the Human Nervous-System and in Neuroblastomas - an Immunohistochemical Study*. International Journal of Oncology, 1993. **3**(5): p. 909-915.
48. Cheever, M.A., et al., *The prioritization of cancer antigens: a national cancer institute pilot project for the acceleration of translational research*. Clin Cancer Res, 2009. **15**(17): p. 5323-37.
49. Yamashiro, S., et al., *Genetic and enzymatic basis for the differential expression of GM2 and GD2 gangliosides in human cancer cell lines*. Cancer Res, 1993. **53**(22): p. 5395-400.
50. Suzuki, M. and N.K.V. Cheung, *Disialoganglioside GD2 as a therapeutic target for human diseases*. Expert Opinion on Therapeutic Targets, 2015. **19**(3): p. 349-362.
51. Furukawa, K., et al., *Disialyl gangliosides enhance tumor phenotypes with differential modalities*. Glycoconj J, 2012. **29**(8-9): p. 579-84.
52. Cheung, N.K., et al., *Key role for myeloid cells: phase II results of anti-G(D2) antibody 3F8 plus granulocyte-macrophage colony-stimulating factor for chemoresistant osteomedullary neuroblastoma*. Int J Cancer, 2014. **135**(9): p. 2199-205.
53. Cheung, N.K., et al., *Murine anti-GD2 monoclonal antibody 3F8 combined with granulocyte-macrophage colony-stimulating factor and 13-cis-retinoic acid in high-risk patients with stage 4 neuroblastoma in first remission*. J Clin Oncol, 2012. **30**(26): p. 3264-70.
54. Cheung, N.K., et al., *Monoclonal antibodies to a glycolipid antigen on human neuroblastoma cells*. Cancer Res, 1985. **45**(6): p. 2642-9.
55. Wu, Z.L., et al., *Expression of GD2 ganglioside by untreated primary human neuroblastomas*. Cancer Res, 1986. **46**(1): p. 440-3.
56. Cheung, N.K., et al., *Targeting of ganglioside GD2 monoclonal antibody to neuroblastoma*. J Nucl Med, 1987. **28**(10): p. 1577-83.
57. Liu, B., et al., *Endothelin A receptor antagonism enhances inhibitory effects of anti-ganglioside GD2 monoclonal antibody on invasiveness and viability of human osteosarcoma cells*. PLoS One, 2014. **9**(4): p. e93576.
58. Imai, M., et al., *Complement-mediated mechanisms in anti-GD2 monoclonal antibody therapy of murine metastatic cancer*. Cancer Res, 2005. **65**(22): p. 10562-8.
59. Sait, S. and S. Modak, *Anti-GD2 immunotherapy for neuroblastoma*. Expert Review of Anticancer Therapy, 2017. **17**(10): p. 889-904.

60. Tsao, C.Y., et al., *Anti-proliferative and pro-apoptotic activity of GD2 ganglioside-specific monoclonal antibody 3F8 in human melanoma cells*. *Oncoimmunology*, 2015. **4**(8): p. e1023975.
61. Cheung, N.K., et al., *Ganglioside GD2 specific monoclonal antibody 3F8: a phase I study in patients with neuroblastoma and malignant melanoma*. *J Clin Oncol*, 1987. **5**(9): p. 1430-40.
62. Isaacs, J.D., J. Greenwood, and H. Waldmann, *Therapy with monoclonal antibodies. II. The contribution of Fc gamma receptor binding and the influence of C(H)1 and C(H)3 domains on in vivo effector function*. *J Immunol*, 1998. **161**(8): p. 3862-9.
63. Baxevanis, C.N., et al., *Granulocyte-macrophage colony-stimulating factor improves immunological parameters in patients with refractory solid tumours receiving second-line chemotherapy: correlation with clinical responses*. *Eur J Cancer*, 1997. **33**(8): p. 1202-8.
64. Jiang, T., C. Zhou, and S. Ren, *Role of IL-2 in cancer immunotherapy*. *Oncoimmunology*, 2016. **5**(6): p. e1163462.
65. Pearson, A.D., et al., *High-dose rapid and standard induction chemotherapy for patients aged over 1 year with stage 4 neuroblastoma: a randomised trial*. *Lancet Oncol*, 2008. **9**(3): p. 247-56.
66. Matthay, K.K., et al., *Long-term results for children with high-risk neuroblastoma treated on a randomized trial of myeloablative therapy followed by 13-cis-retinoic acid: a children's oncology group study*. *J Clin Oncol*, 2009. **27**(7): p. 1007-13.
67. Mueller, B.M., et al., *Enhancement of antibody-dependent cytotoxicity with a chimeric anti-GD2 antibody*. *J Immunol*, 1990. **144**(4): p. 1382-6.
68. Ozkaynak, M.F., et al., *Phase I study of chimeric human/murine anti-ganglioside G(D2) monoclonal antibody (ch14.18) with granulocyte-macrophage colony-stimulating factor in children with neuroblastoma immediately after hematopoietic stem-cell transplantation: a Children's Cancer Group Study*. *J Clin Oncol*, 2000. **18**(24): p. 4077-85.
69. Gilman, A.L., et al., *Phase I study of ch14.18 with granulocyte-macrophage colony-stimulating factor and interleukin-2 in children with neuroblastoma after autologous bone marrow transplantation or stem-cell rescue: a report from the Children's Oncology Group*. *J Clin Oncol*, 2009. **27**(1): p. 85-91.
70. Simon, T., et al., *Long term outcome of high-risk neuroblastoma patients after immunotherapy with antibody ch14.18 or oral metronomic chemotherapy*. *BMC Cancer*, 2011. **11**: p. 21.
71. Buettner, M.J., et al., *Improving Immunotherapy Through Glycodesign*. *Frontiers in Immunology*, 2018. **9**.
72. Ladenstein, R., et al., *Ch14.18 antibody produced in CHO cells in relapsed or refractory Stage 4 neuroblastoma patients: a SIOPEN Phase 1 study*. *MAbs*, 2013. **5**(5): p. 801-9.
73. Zeng, Y., et al., *Anti-neuroblastoma effect of ch14.18 antibody produced in CHO cells is mediated by NK-cells in mice*. *Molecular Immunology*, 2005. **42**(11): p. 1311-1319.
74. Xiao, W.H., A.L. Yu, and L.S. Sorkin, *Electrophysiological characteristics of primary afferent fibers after systemic administration of anti-GD2 ganglioside antibody*. *Pain*, 1997. **69**(1-2): p. 145-51.
75. Mueller, I., et al., *Tolerability, response and outcome of high-risk neuroblastoma patients treated with long-term infusion of anti-GD2 antibody ch14.18/CHO*. *MAbs*, 2018. **10**(1): p. 55-61.

76. Siebert, N., et al., *Pharmacokinetics and pharmacodynamics of ch14.18/CHO in relapsed/refractory high-risk neuroblastoma patients treated by long-term infusion in combination with IL-2*. *MABs*, 2016. **8**(3): p. 604-16.
77. Keyel, M.E. and C.P. Reynolds, *Spotlight on dinutuximab in the treatment of high-risk neuroblastoma: development and place in therapy*. *Biologics*, 2019. **13**: p. 1-12.
78. Ladenstein, R., et al., *Interleukin 2 with anti-GD2 antibody ch14.18/CHO (dinutuximab beta) in patients with high-risk neuroblastoma (HR-NBL1/SIOPEX): a multicentre, randomised, phase 3 trial*. *Lancet Oncol*, 2018. **19**(12): p. 1617-1629.
79. Matthay, K.K., *Interleukin 2 plus anti-GD2 immunotherapy: helpful or harmful?* *Lancet Oncol*, 2018. **19**(12): p. 1549-1551.
80. Ladenstein, R., et al., *Investigation of the Role of Dinutuximab Beta-Based Immunotherapy in the SIOPEX High-Risk Neuroblastoma 1 Trial (HR-NBL1)*. *Cancers (Basel)*, 2020. **12**(2).
81. Ladenstein, R., et al., *Investigation of the Role of Dinutuximab Beta-Based Immunotherapy in the SIOPEX High-Risk Neuroblastoma 1 Trial (HR-NBL1)*. *Cancers*, 2020. **12**(2).
82. Keller, D. *IL-2 adds only toxicity to neuroblastoma antibody treatment*. in *ASCO Annual Meeting*. 2016. Chicago
83. Galili, U., *The alpha-gal epitope and the anti-Gal antibody in xenotransplantation and in cancer immunotherapy*. *Immunol Cell Biol*, 2005. **83**(6): p. 674-86.
84. Siebert, N., et al., *Validated detection of anti-GD2 antibody ch14.18/CHO in serum of neuroblastoma patients using anti-idiotypic antibody ganglidiomab*. *J Immunol Methods*, 2013. **398-399**: p. 51-9.
85. Siebert, N., et al., *Validated detection of human anti-chimeric immune responses in serum of neuroblastoma patients treated with ch14.18/CHO*. *Journal of Immunological Methods*, 2014. **407**: p. 108-115.
86. Siebert, N., et al., *Impact of HACA on Immunomodulation and Treatment Toxicity Following ch14.18/CHO Long-Term Infusion with Interleukin-2: Results from a SIOPEX Phase 2 Trial*. *Cancers (Basel)*, 2018. **10**(10).
87. Ragupathi, G., et al., *Consistent antibody response against ganglioside GD2 induced in patients with melanoma by a GD2 lactone-keyhole limpet hemocyanin conjugate vaccine plus immunological adjuvant QS-21*. *Clin Cancer Res*, 2003. **9**(14): p. 5214-20.
88. Zhang, H., et al., *Antibodies against GD2 ganglioside can eradicate syngeneic cancer micrometastases*. *Cancer Research*, 1998. **58**(13): p. 2844-2849.
89. Tong, W.Y., et al., *Vaccination with Tumor-Ganglioside Glycomimetics Activates a Selective Immunity that Affords Cancer Therapy*. *Cell Chemical Biology*, 2019. **26**(7): p. 1013-+.
90. Grayson, G. and S. Ladisch, *Immunosuppression by human gangliosides. II. Carbohydrate structure and inhibition of human NK activity*. *Cell Immunol*, 1992. **139**(1): p. 18-29.
91. Caldwell, S., et al., *Mechanisms of ganglioside inhibition of APC function*. *Journal of Immunology*, 2003. **171**(4): p. 1676-1683.
92. Poon, V.I., et al., *Ganglioside GD2 expression is maintained upon recurrence in patients with osteosarcoma*. *Clinical Sarcoma Research*, 2015. **5**.
93. Sun, L.N., et al., *Carbohydrates as T-cell antigens with implications in health and disease*. *Glycobiology*, 2016. **26**(10): p. 1029-1040.
94. Ragupathi, G., et al., *Consistent antibody response against ganglioside GD2 induced in patients with melanoma by a GD2 lactone-keyhole limpet hemocyanin conjugate*

- vaccine plus immunological adjuvant QS-21*. *Clinical Cancer Research*, 2003. **9**(14): p. 5214-5220.
95. Kushner, B.H., et al., *Phase I trial of a bivalent gangliosides vaccine in combination with beta-glucan for high-risk neuroblastoma in second or later remission*. *Clin Cancer Res*, 2014. **20**(5): p. 1375-82.
 96. Astronomo, R.D. and D.R. Burton, *Carbohydrate vaccines: developing sweet solutions to sticky situations?* *Nat Rev Drug Discov*, 2010. **9**(4): p. 308-24.
 97. Barral, D.C. and M.B. Brenner, *CD1 antigen presentation: how it works*. *Nat Rev Immunol*, 2007. **7**(12): p. 929-41.
 98. Chapman, P.B., et al., *A phase II trial comparing five dose levels of BEC2 anti-idiotypic monoclonal antibody vaccine that mimics GD3 ganglioside*. *Vaccine*, 2004. **22**(21-22): p. 2904-2909.
 99. Tong, W., et al., *Small-molecule ligands of GD2 ganglioside, designed from NMR studies, exhibit induced-fit binding and bioactivity*. *Chem Biol*, 2010. **17**(2): p. 183-94.
 100. Lebecque, S., et al., *Immunologic characterization of monoclonal antibodies that modulate human IgE binding to the major birch pollen allergen Bet v 1*. *J Allergy Clin Immunol*, 1997. **99**(3): p. 374-84.
 101. Aghebati-Maleki, L., et al., *Phage display as a promising approach for vaccine development*. *Journal of Biomedical Science*, 2016. **23**.
 102. Alfaleh, M.A., et al., *Phage Display Derived Monoclonal Antibodies: From Bench to Bedside*. *Front Immunol*, 2020. **11**: p. 1986.
 103. Fest, S., et al., *GD2 peptide mimotope DNA vaccines for anti-neuroblastoma immunotherapy*. *Blood*, 2004. **104**(11): p. 379a-380a.
 104. Fest, S., et al., *Characterization of GD2 peptide mimotope DNA vaccines effective against spontaneous neuroblastoma metastases*. *Cancer Res*, 2006. **66**(21): p. 10567-75.
 105. Hilpert, K., D.F. Winkler, and R.E. Hancock, *Peptide arrays on cellulose support: SPOT synthesis, a time and cost efficient method for synthesis of large numbers of peptides in a parallel and addressable fashion*. *Nat Protoc*, 2007. **2**(6): p. 1333-49.
 106. Bleeke, M., et al., *Systematic amino acid substitutions improved efficiency of GD(2)-peptide mimotope vaccination against neuroblastoma*. *European Journal of Cancer*, 2009. **45**(16): p. 2915-2921.
 107. Nisonoff, A. and E. Lamoyi, *Implications of the presence of an internal image of the antigen in anti-idiotypic antibodies: possible application to vaccine production*. *Clin Immunol Immunopathol*, 1981. **21**(3): p. 397-406.
 108. Jerne, N.K., *Towards a network theory of the immune system*. *Ann Immunol (Paris)*, 1974. **125C**(1-2): p. 373-89.
 109. Gajdosik, Z., *Racotumomab - a novel anti-idiotypic monoclonal antibody vaccine for the treatment of cancer*. *Drugs Today (Barc)*, 2014. **50**(4): p. 301-7.
 110. Ladjemi, M.Z., *Anti-idiotypic antibodies as cancer vaccines: achievements and future improvements*. *Front Oncol*, 2012. **2**: p. 158.
 111. Herlyn, D., et al., *Anti-idiotypic cancer vaccines: past and future*. *Cancer Immunol Immunother*, 1996. **43**(2): p. 65-76.
 112. Bhattacharya-Chatterjee, M., S.K. Chatterjee, and K.A. Foon, *Anti-idiotypic vaccine against cancer*. *Immunol Lett*, 2000. **74**(1): p. 51-8.
 113. Mittelman, A., et al., *Active specific immunotherapy in patients with melanoma. A clinical trial with mouse antiidiotypic monoclonal antibodies elicited with syngeneic*

- anti-high-molecular-weight-melanoma-associated antigen monoclonal antibodies.* J Clin Invest, 1990. **86**(6): p. 2136-44.
114. Mittelman, A., et al., *Human high molecular weight melanoma-associated antigen (HMW-MAA) mimicry by mouse anti-idiotypic monoclonal antibody MK2-23: induction of humoral anti-HMW-MAA immunity and prolongation of survival in patients with stage IV melanoma.* Proc Natl Acad Sci U S A, 1992. **89**(2): p. 466-70.
 115. Berthold, F., *NB2004 Trial Protocol* Identifier: NCT00410631, 2004. <https://clinicaltrials.gov/ct2/show/record/NCT00410631>.
 116. Smith, V. and J. Foster, *High-Risk Neuroblastoma Treatment Review.* Children (Basel), 2018. **5**(9).
 117. Corbacioglu, S., et al., *The RIST design: A molecularly targeted multimodal approach for the treatment of patients with relapsed and refractory neuroblastoma.* Journal of Clinical Oncology, 2013. **31**(15_suppl): p. 10017-10017.
 118. Illhardt, T., et al., *Haploidentical Stem Cell Transplantation for Refractory/Relapsed Neuroblastoma.* Biol Blood Marrow Transplant, 2018. **24**(5): p. 1005-1012.
 119. Siebert, N., et al., *Validated detection of human anti-chimeric immune responses in serum of neuroblastoma patients treated with ch14.18/CHO.* J Immunol Methods, 2014. **407**: p. 108-15.
 120. Eger, C., et al., *Generation and Characterization of a Human/Mouse Chimeric GD2-Mimicking Anti-Idiotypic Antibody Ganglidximab for Active Immunotherapy against Neuroblastoma.* PLoS One, 2016. **11**(3): p. e0150479.
 121. Siebert, N., et al., *Functional bioassays for immune monitoring of high-risk neuroblastoma patients treated with ch14.18/CHO anti-GD2 antibody.* PLoS One, 2014. **9**(9): p. e107692.
 122. Glen, S. *Grubbs' Test for Outliers.* 2016 [cited 2021 March 26]; Available from: <https://www.statisticshowto.com/grubbs-test/>.
 123. Casey, D.L. and N.V. Cheung, *Immunotherapy of Pediatric Solid Tumors: Treatments at a Crossroads, with an Emphasis on Antibodies.* Cancer Immunol Res, 2020. **8**(2): p. 161-166.
 124. Kaplon, H. and J.M. Reichert, *Antibodies to watch in 2021.* MAbs, 2021. **13**(1): p. 1860476.
 125. Mora, J., et al., *Naxitamab, a new generation anti-GD2 monoclonal antibody (mAb) for treatment of relapsed/refractory high-risk neuroblastoma (HR-NB).* Journal of Clinical Oncology, 2020. **38**(15_suppl): p. 10543-10543.
 126. Park, J.A. and N.-K.V. Cheung, *Targets and Antibody Formats for Immunotherapy of Neuroblastoma.* Journal of Clinical Oncology, 2020. **38**(16): p. 1836-1848.
 127. Szanto, C.L., et al., *Monitoring Immune Responses in Neuroblastoma Patients during Therapy.* Cancers (Basel), 2020. **12**(2).
 128. Siebert, N., et al., *PD-1 blockade augments anti-neuroblastoma immune response induced by anti-GD2 antibody ch14.18/CHO.* Oncoimmunology, 2017. **6**(10): p. e1343775.
 129. Ehlert, K., et al., *Nivolumab and dinutuximab beta in two patients with refractory neuroblastoma.* J Immunother Cancer, 2020. **8**(1).
 130. Richards, R.M., E. Sotillo, and R.G. Majzner, *CAR T Cell Therapy for Neuroblastoma.* Front Immunol, 2018. **9**: p. 2380.
 131. Straathof, K., et al., *Antitumor activity without on-target off-tumor toxicity of GD2-chimeric antigen receptor T cells in patients with neuroblastoma.* Sci Transl Med, 2020. **12**(571).

132. Cheung, I.Y., et al., *Survival Impact of Anti-GD2 Antibody Response in a Phase II Ganglioside Vaccine Trial Among Patients With High-Risk Neuroblastoma With Prior Disease Progression*. J Clin Oncol, 2021. **39**(3): p. 215-226.
133. Bremm, M., et al., *Generation and flow cytometric quality control of clinical-scale TCRalphabeta/CD19-depleted grafts*. Cytometry B Clin Cytom, 2017. **92**(2): p. 126-135.
134. Corre, E., et al., *Long-term immune deficiency after allogeneic stem cell transplantation: B-cell deficiency is associated with late infections*. Haematologica, 2010. **95**(6): p. 1025-1029.
135. Jason-Moller, L., M. Murphy, and J. Bruno, *Overview of Biacore systems and their applications*. Curr Protoc Protein Sci, 2006. **Chapter 19**: p. Unit 19.13.
136. Schneider, C.S., et al., *Surface plasmon resonance as a high throughput method to evaluate specific and non-specific binding of nanotherapeutics*. Journal of controlled release : official journal of the Controlled Release Society, 2015. **219**: p. 331-344.
137. Petrovsky, N., *Comparative Safety of Vaccine Adjuvants: A Summary of Current Evidence and Future Needs*. Drug Safety, 2015. **38**(11): p. 1059-1074.
138. Harris, J.R., et al., *Alhydrogel (R) adjuvant, ultrasonic dispersion and protein binding: A TEM and analytical study*. Micron, 2012. **43**(2-3): p. 192-200.
139. Chang, J.C.C., et al., *Adjuvant activity of incomplete Freund's adjuvant*. Advanced Drug Delivery Reviews, 1998. **32**(3): p. 173-186.
140. Slingluff, C.L., et al., *Immunogenicity for CD8+ and CD4+ T cells of 2 formulations of an incomplete freund's adjuvant for multi-peptide melanoma vaccines*. Journal of immunotherapy (Hagerstown, Md. : 1997), 2010. **33**(6): p. 630-638.
141. Melssen, M.M., et al., *A multi-peptide vaccine plus toll-like receptor agonists LPS or poly(I:CLC) in combination with incomplete Freund's adjuvant in melanoma patients*. J Immunother Cancer, 2019. **7**(1): p. 163.
142. Vetvicka, V., L. Vannucci, and P. Sima, *beta-glucan as a new tool in vaccine development*. Scandinavian Journal of Immunology, 2020. **91**(2).
143. Goodridge, H.S., A.J. Wolf, and D.M. Underhill, *beta-glucan recognition by the innate immune system*. Immunological Reviews, 2009. **230**: p. 38-50.
144. Hilpert, K., D.F.H. Winkler, and R.E.W. Hancock, *Peptide arrays on cellulose support: SPOT synthesis, a time and cost efficient method for synthesis of large numbers of peptides in a parallel and addressable fashion*. Nature Protocols, 2007. **2**(6): p. 1333-1349.
145. Knittelfelder, R., A.B. Riemer, and E. Jensen-Jarolim, *Mimotope vaccination - from allergy to cancer*. Expert Opinion on Biological Therapy, 2009. **9**(4): p. 493-506.
146. Forster-Waldl, E., et al., *Isolation and structural analysis of peptide mimotopes for the disialoganglioside GD2, a neuroblastoma tumor antigen*. Mol Immunol, 2005. **42**(3): p. 319-25.
147. Bolesta, E., et al., *DNA vaccine expressing the mimotope of GD2 ganglioside induces protective GD2 cross-reactive antibody responses*. Cancer Res, 2005. **65**(8): p. 3410-8.
148. Tobias, J., et al., *A New Strategy Toward B Cell-Based Cancer Vaccines by Active Immunization With Mimotopes of Immune Checkpoint Inhibitors*. Front Immunol, 2020. **11**: p. 895.
149. London, W.B., et al., *Historical time to disease progression and progression-free survival in patients with recurrent/refractory neuroblastoma treated in the modern era on Children's Oncology Group early-phase trials*. Cancer, 2017. **123**(24): p. 4914-4923.

8. Danksagung

Ein besonderes Wort des Dankes geht an Prof. Dr. med. Holger Lode für die Überlassung des interessanten Themas. Mit vielen wertvollen Hinweisen und Anregungen konnte diese Arbeit entstehen.

Ferner möchte ich mich bei allen Mitgliedern der Arbeitsgruppe pädiatrische Onkologie bedanken, insbesondere Dr. Nikolai Siebert, Dr. Sascha Troschke Meurer sowie die technischen Assistent*Innen Theodor Köpp und Maria Asmus, deren frühere Veröffentlichungen und Arbeiten zum Gelingen dieser Arbeit beigetragen haben.

Ein besonderer Dank geht auch an die Patienten und ihre Familien, deren Mut und Hoffnung für diese Arbeit unersetzlich waren.

Zuletzt möchte ich mich bei meiner Familie und meinen Freunden bedanken, die mich trotz der Distanz zwischen uns in den letzten Jahren unterstützt und ermutigt haben. Ihr seid die beste Familie und Freunde, die man sich nur wünschen kann.

9. Eidesstattliche Erklärung

Hiermit versichere ich, dass ich die vorliegende Dissertation selbständig verfasst und keine anderen als die angegebenen Hilfsmittel verwendet habe.

Die Dissertation ist bisher an keiner anderen Fakultät und keiner anderen wissenschaftlichen Einrichtung vorgelegt worden.

Ich erkläre, dass ich bisher kein anderes Promotionsverfahren erfolglos beendet habe und dass eine Aberkennung eines bereits erworbenen Dokortitels nicht vorliegt.

Ort, Datum

Leah Klingel

10. Lebenslauf

Persönliche Daten	
Name	Leah Bernadette Klingel
E-Mail-Adresse	leah.klingel@uni-greifswald.de
Staatsangehörigkeit	Philippinische
Sprachkenntnisse	Englisch, Filipino: Muttersprache Deutsch: Fortgeschritten
Berufliche Erfahrungen	
Mai 2018 bis aktuell	Assistenzärztin in der Klinik für Kinder- und Jugendmedizin, Universitätsmedizin Greifswald
März 2016 - November 2017	Programmmanagerin <i>Kalusugan ng Mag-ina</i> Alliance for Improving Health Outcomes, Inc. Manila, Philippinen
März 2014 - August 2014	Kinderärztin im Dienst Manila, Philippinen
Mai 2014 - September 2014	Lehrkraft für Psychologie De La Salle University Manila, Philippinen
Januar 2011 - Dezember 2013	Assistenzärztin Pädiatrie Philippine Children's Medical Center Manila, Philippinen
Ausbildung	
Februar 2015 - September 2015	MSc International Health (Erasmus Mundus Scholar) Institute for Global Health, University College London London, Vereinigtes Königreich
August 2014 - Januar 2015	MSc International Health (Erasmus Mundus Scholar) Institut für Tropenmedizin und Internationale Gesundheit, Charité-Universitätsmedizin Berlin Berlin, Deutschland
Juni 2005 - April 2010	Doktor der Medizin University of the Philippines Manila Manila, Philippinen
Juni 2001 - April 2005	Bachelor of Science in Psychologie University of the Philippines Diliman
Juni 1997 - März 2001	Sekundarausbildung (Secondary Education) Francisco Q. Duque Medical Foundation Special Science High School

Poster Präsentation

Presenter, Poster Symposium, 2014 Annual Pediatric Academic Societies and Asian Society for Pediatric Research Meeting in Vancouver, Canada

Research: Scoring System to Predict Mortality Among Children <5 years old Admitted for Pediatric Community Acquired Pneumonia at the Acute Care Unit of the Philippine Children's Medical Center

Master Arbeit

Determining the Effectiveness of the Pneumonia Case Management using the IMCI classification among Malawian children: a secondary data analysis

Thesis Advisor: Timothy Colbourn, BSc Hons, MSc, PhD
Professor of Global Health Systems, Epidemiology and Evaluation
Institute for Global Health, University College London

Ort, Datum

Leah Klingel